AX-PET from demonstrator towards a full-ring brain scanner

Paola Solevi
on behalf of the AX-PET collaboration

IFIC (CSIC/UV), Spain and EBG MedAustron, Austria
paola.solevi@ific.uv.es

The AX-PET collaboration

Great team!

Extraordinary example of technology transfer from High Energy Physics to Medical Physics.

The goal of the AX-PET collaboration

✔ Build and fully characterize a **demonstrator** of a PET camera with 3D localization of the gamma interaction point, decoupling spatial resolution from sensitivity.

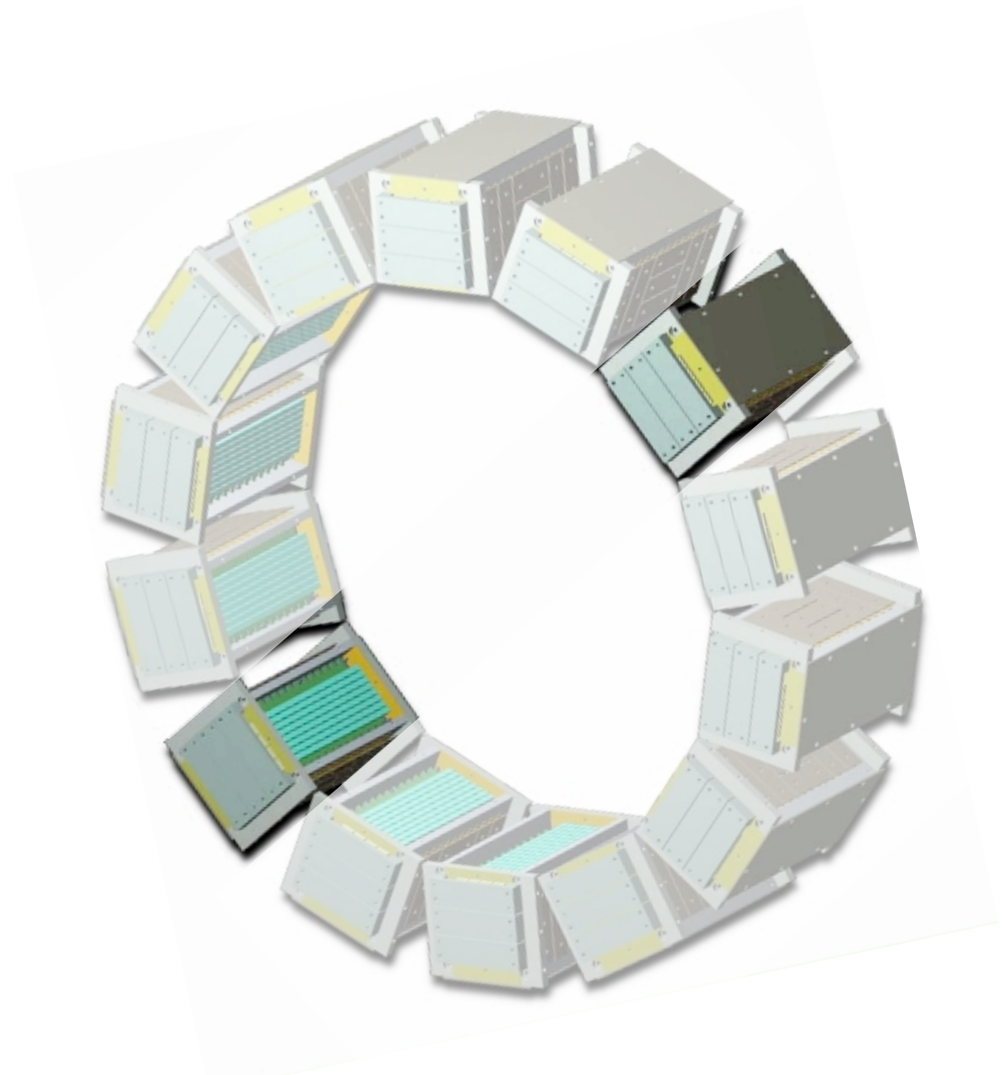

Different PET detector concepts

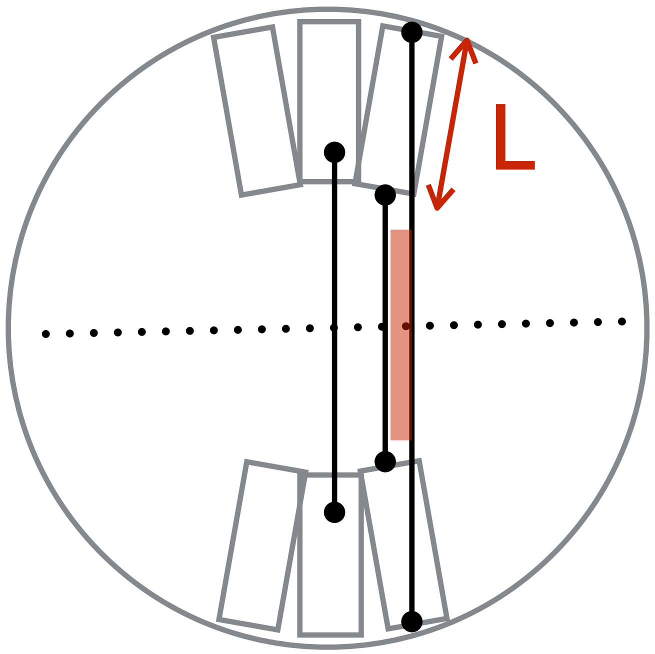

DOI dependence on crystal thickness

	Small crystals	Big crystals
Sensitivity	☹	☺
Resolution	☺	☹

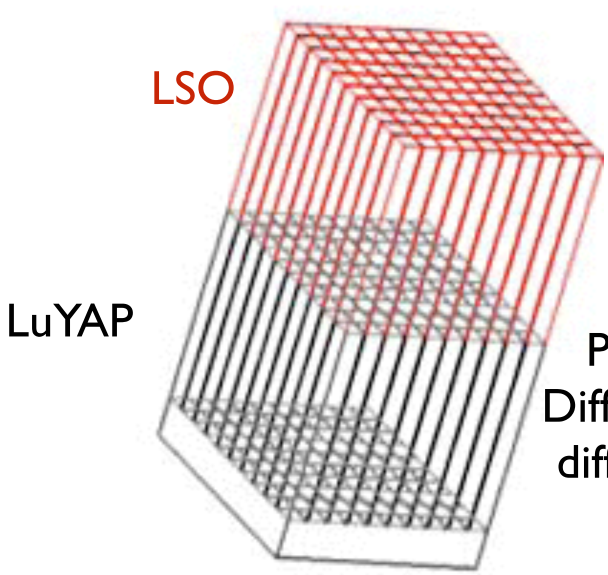

Phoswich scheme
Different crystals with
different decay times

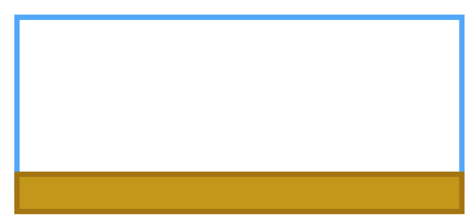

Monolithic scintillator with
pixellated read-out.

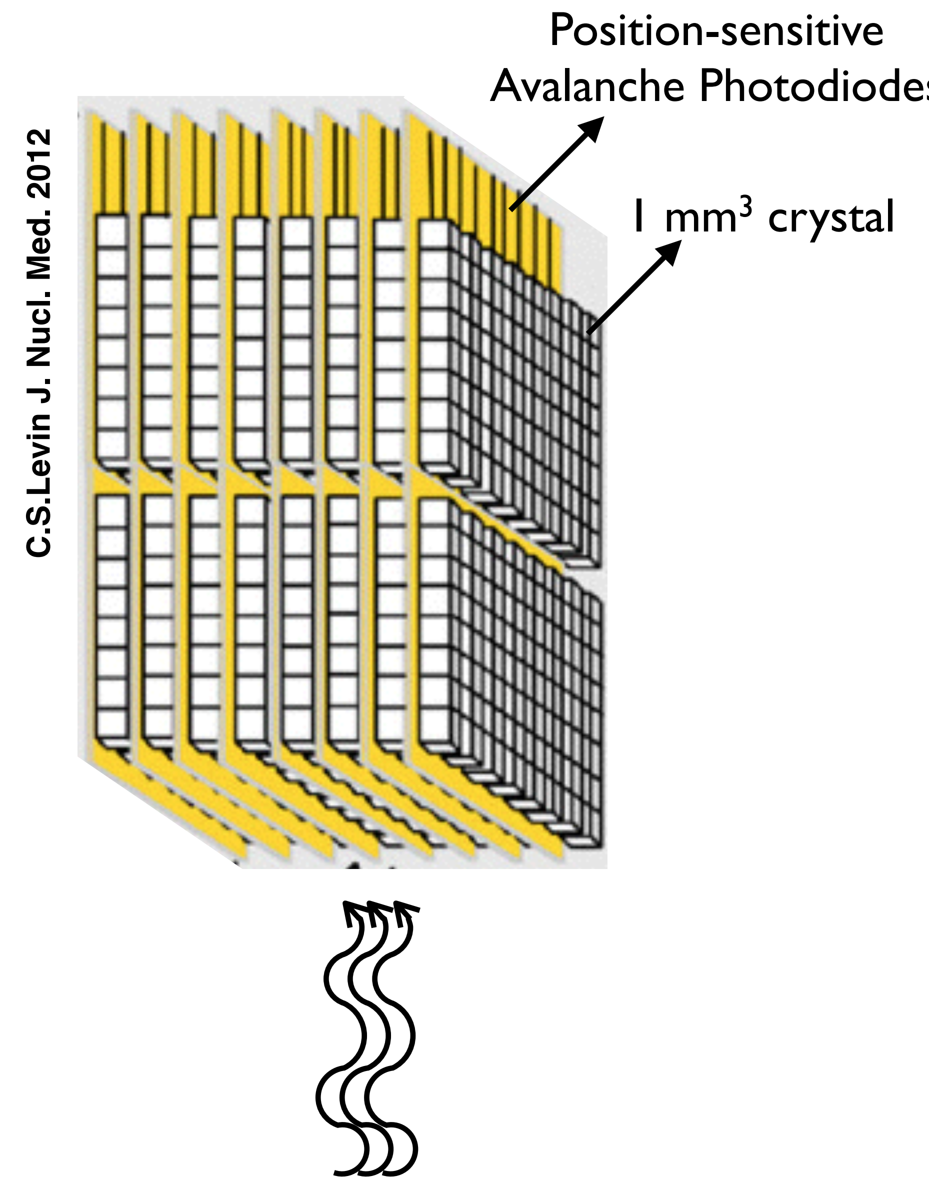

The AX-PET concept

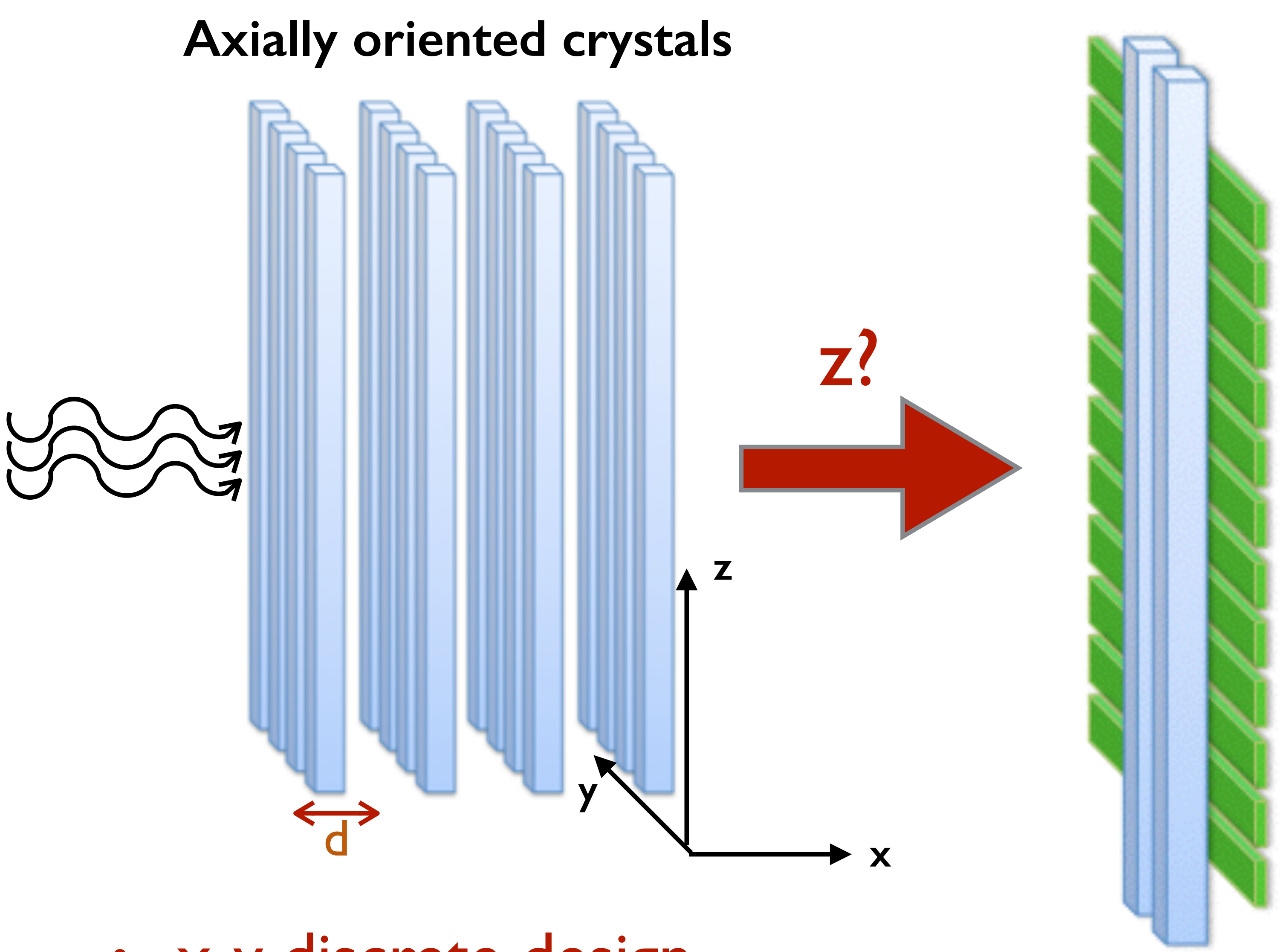

- x-y discrete design
- Trans-axial resolution $\sigma = d/\sqrt{12}$

Hodoscope of WLS strips placed underneath each crystal layer.

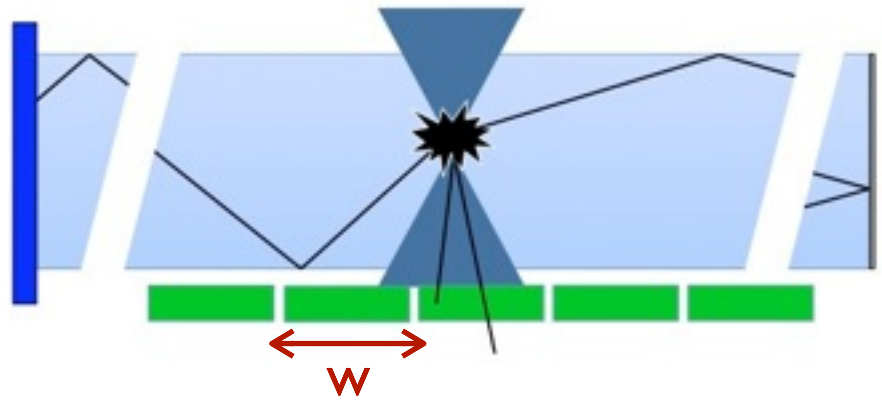

- N≥1 strips fired per event.
- Minimum resolution in z $\sigma = w/\sqrt{12}$

The AX-PET concept

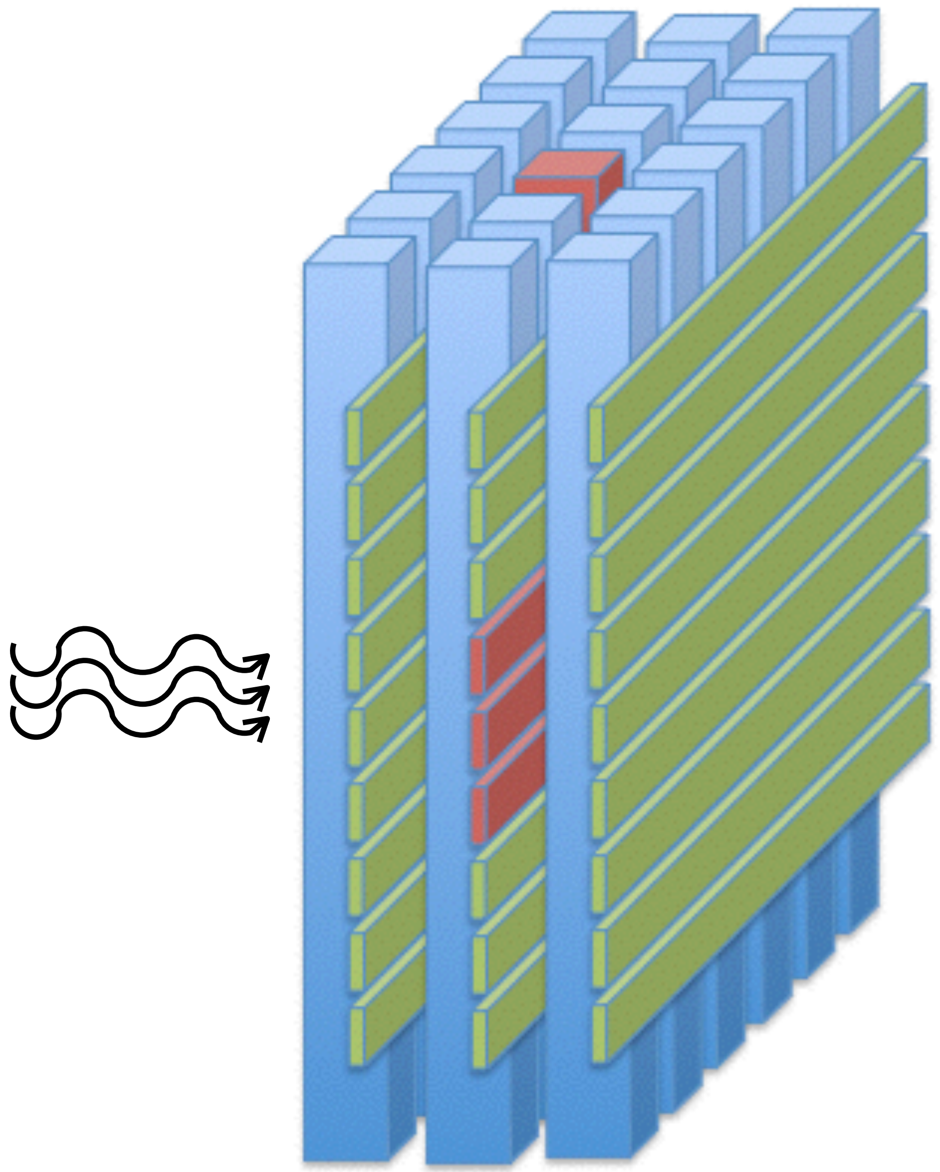

✔ **3D localization** of the gamma interaction with discrete trans-axial coordinate and continuous z.

✔ **High resolution** with mitigated DOI effect.

✔ **Fully scalable** design that can be adapted to different scenario requirements.

The AX-PET module

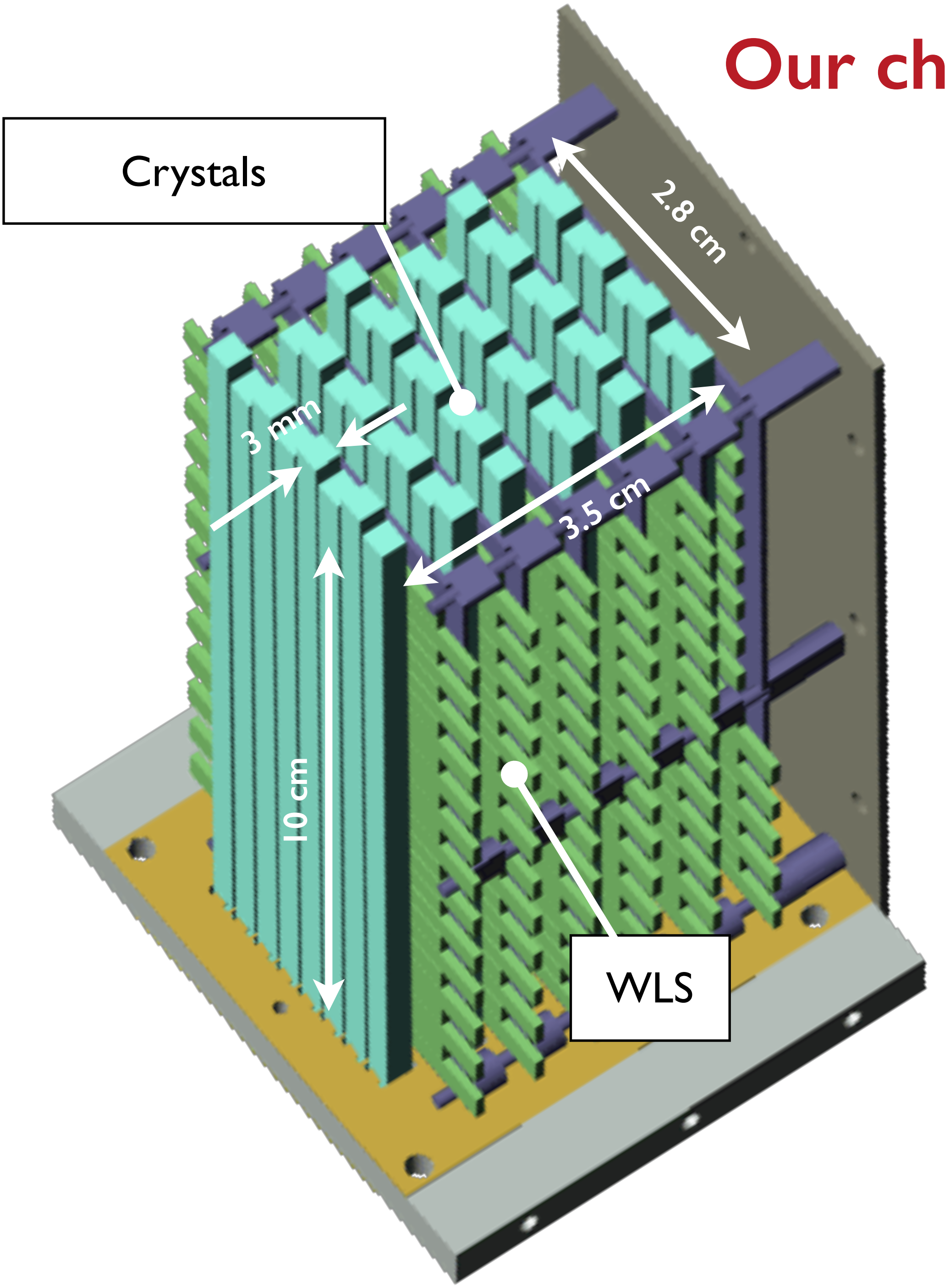

Our choice! Originally conceived for brain imaging.

- 6 layers
- 8 crystals per layer
- 26 WLS strips interleaved to each layer

48 crystals + 156 WLS strips = 204 read-out channels

Alternate individual read-out to guarantee compactness

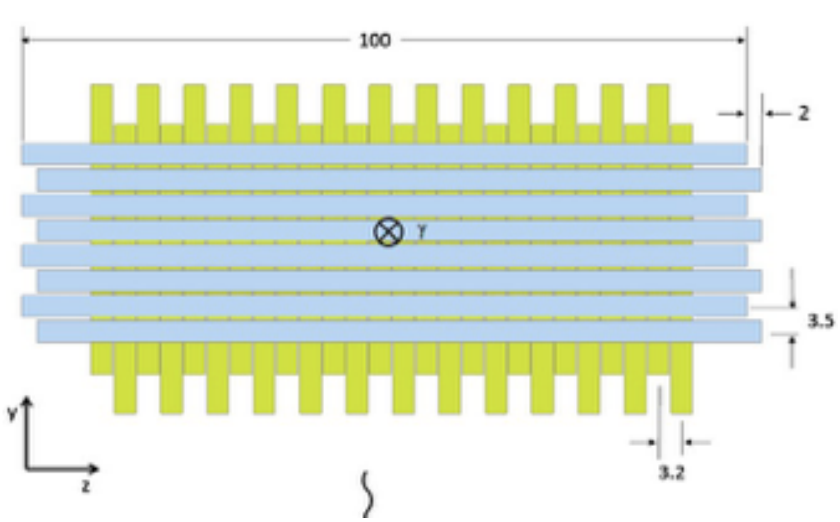

Staggering of crystals to achieve more homogeneous sampling (smaller gaps)

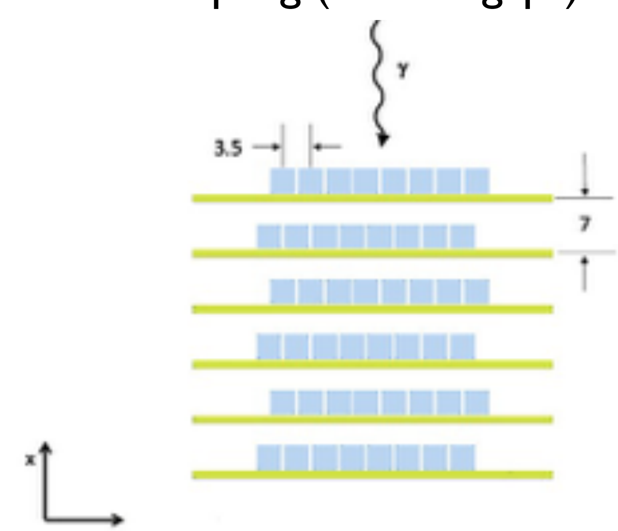

Detection elements

LYSO crystals ($Lu_{1.8}Y_{0.2}SiO_5$: Ce) Prelude 420 from **Saint Gobain**
- 3x3x100 mm^3 read-out on one side
- Aluminum coated on the opposite side to enhance reflectivity ~85%
- Intrinsic resolution (8.3 ± 0.5)% FWHM @511 keV

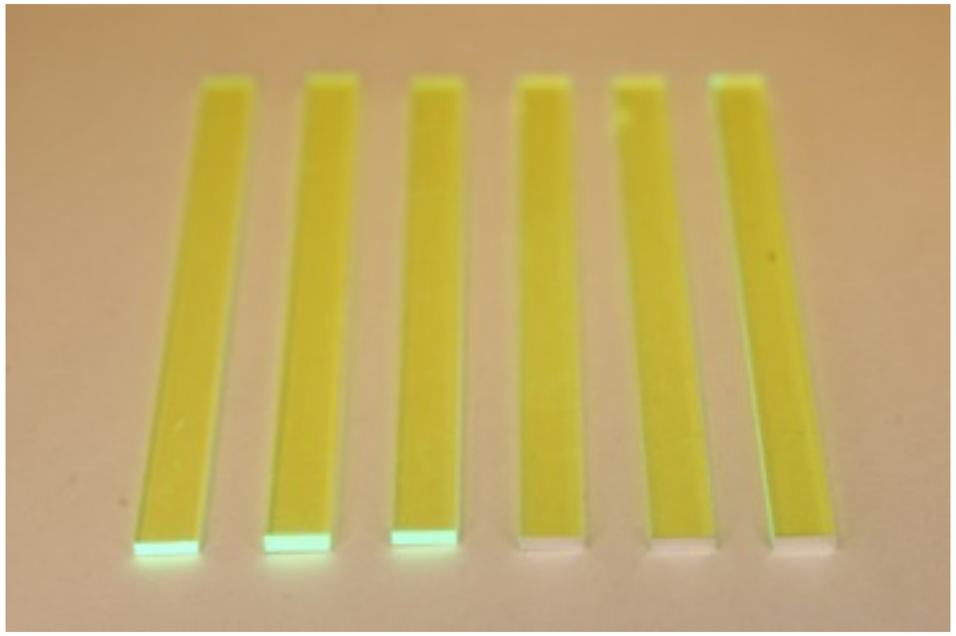

EJ-280-10x from **Eljen Technology**
- 3x0.9x40 mm^3 read-out on one side
- Decay time 8.5 ns
- λ_{blue} = 0.4 mm (highly doped 10x) λ_{green} = 188 mm

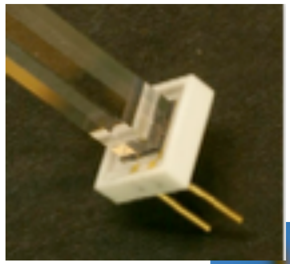

LYSO

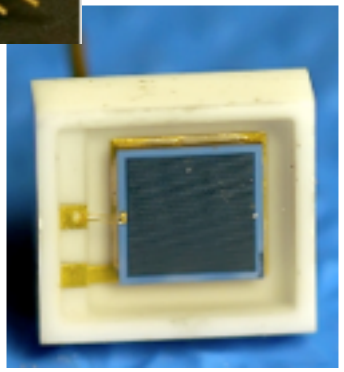

WLS

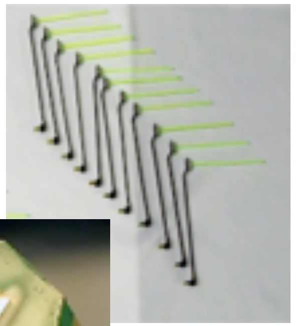

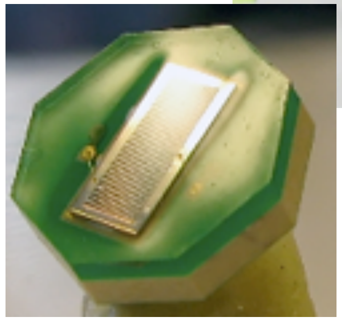

MPPC 3.22×1.19 Octagon-SMD
- 1.2 x 3.2 mm^2 active area
- 782 pixels
- custom made units
- ~40% PDE
- ~1000 pe @ 511 keV

MPPC S10362-33-050C
- 3x3 mm^2 active area
- 3600 pixels
- ~40% PDE
- ~10-50 pe @ 511 keV in LYSO

The AX-PET demonstrator

Two fully assembled modules at CERN.

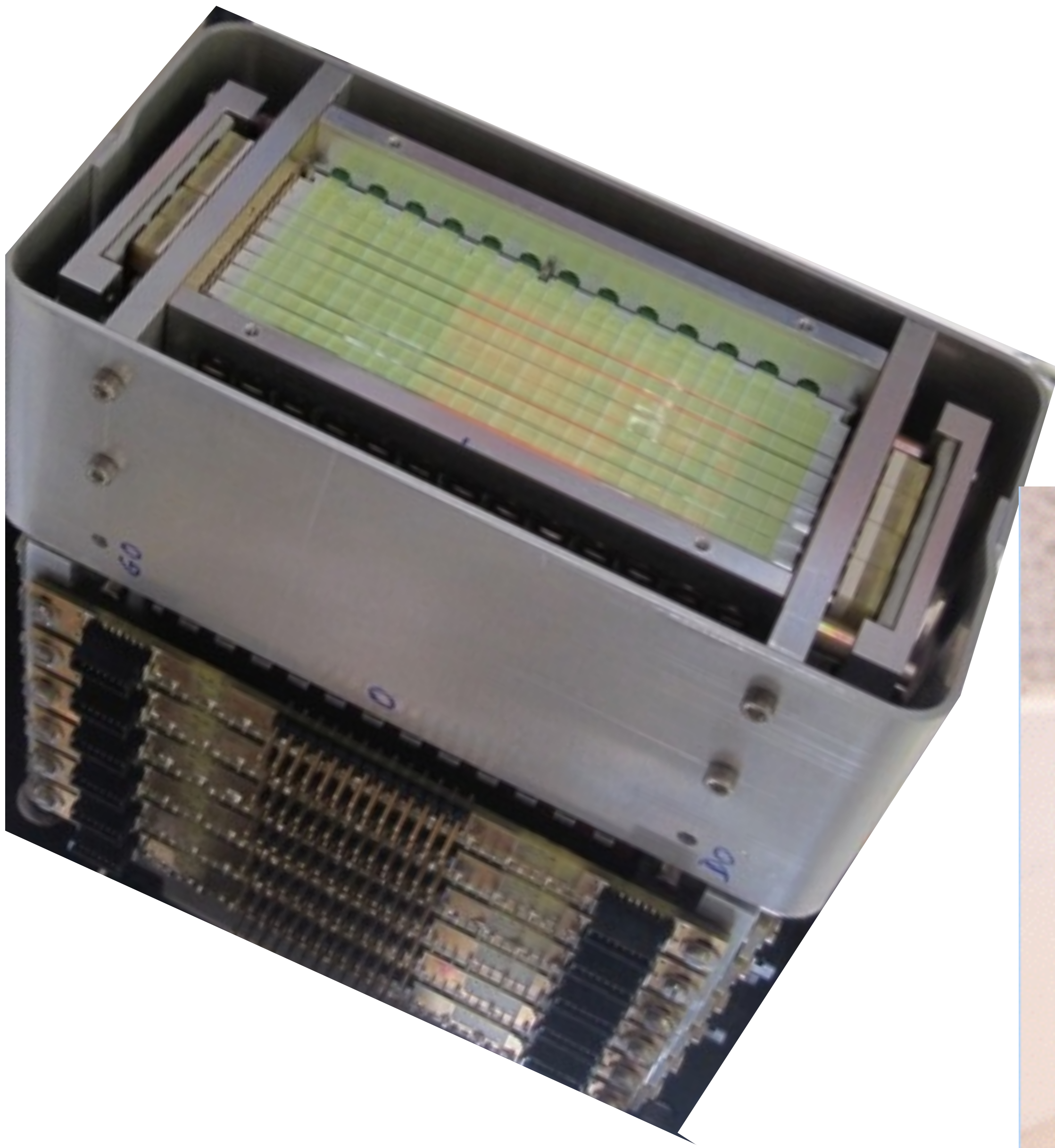

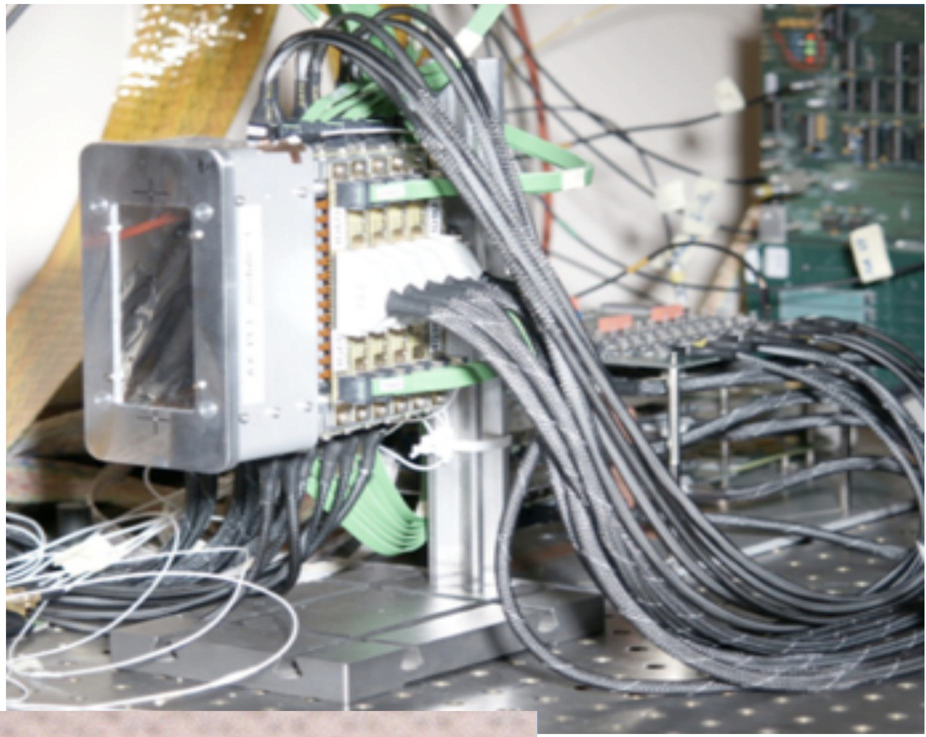

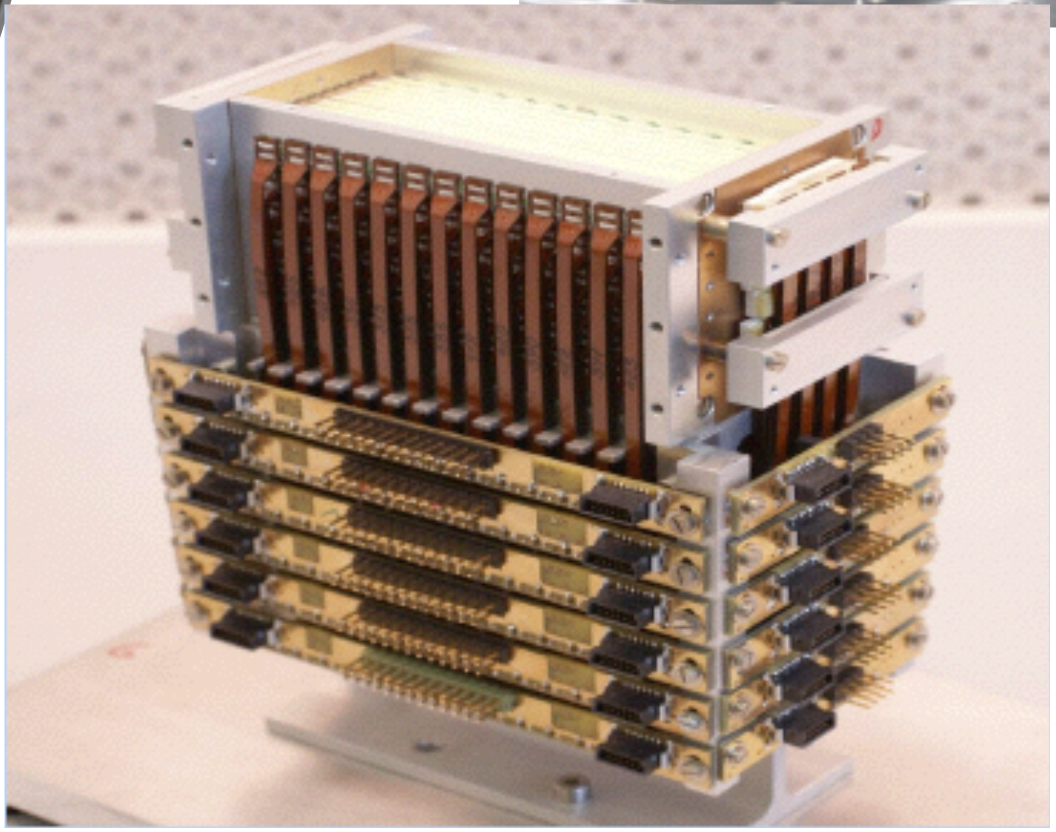

The AX-PET demonstrator

DAQ & Readout Electronics

- Individual analogue readout of MPPC output
- External trigger (NIM logic) to sort coincidences
    - Single crystal **E > 50 keV**
    - Module energy E_sum[400 keV, 600 keV]

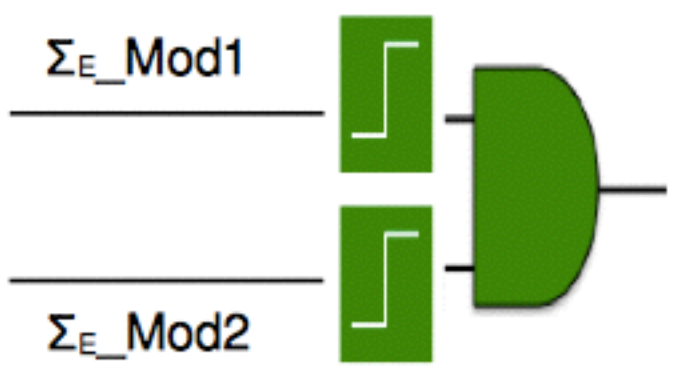

Single crystal energy spectrum in coincidence

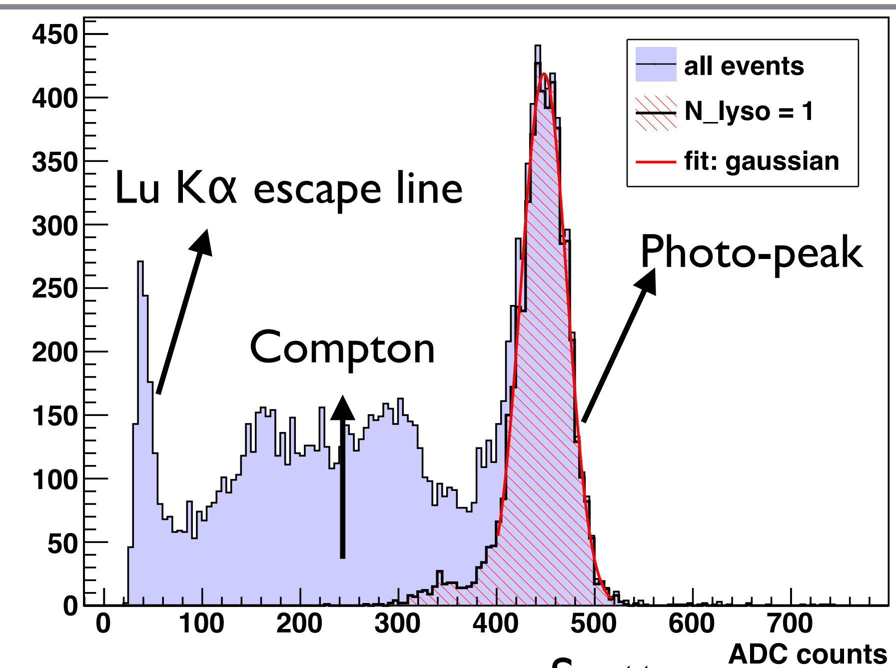

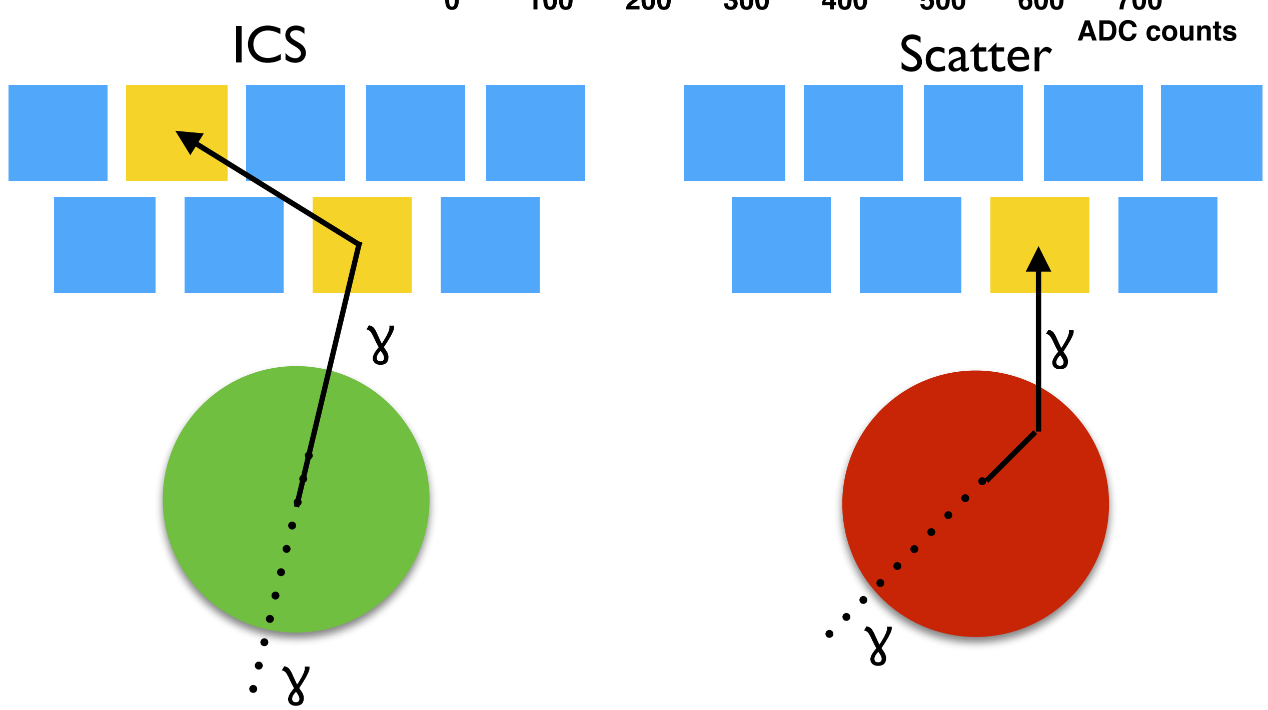

- Scatter in patient rejected
- Inter-Crystal scatter events accepted

Detector calibration and energy resolution

Internal trigger - no source

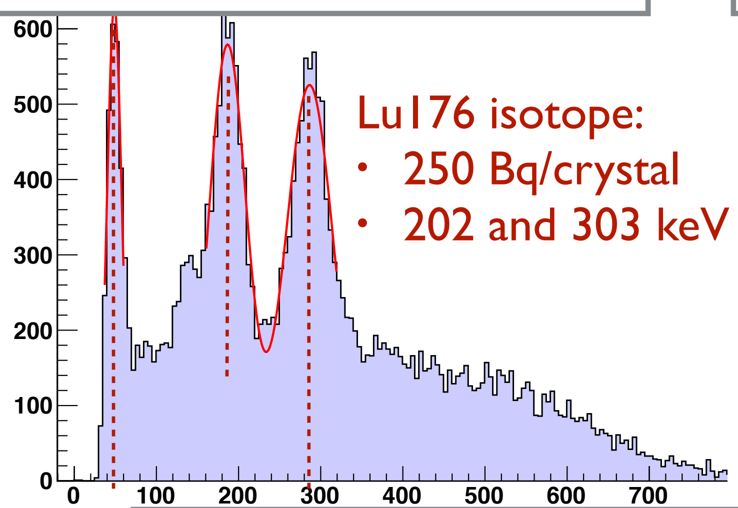

Lu176 isotope:
- 250 Bq/crystal
- 202 and 303 keV

External trigger - Na22 source

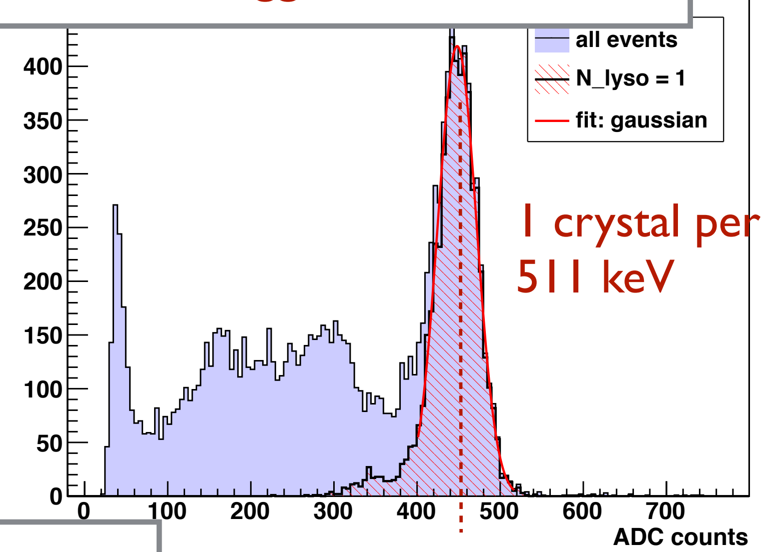

1 crystal per module
511 keV

Typical calibration curve

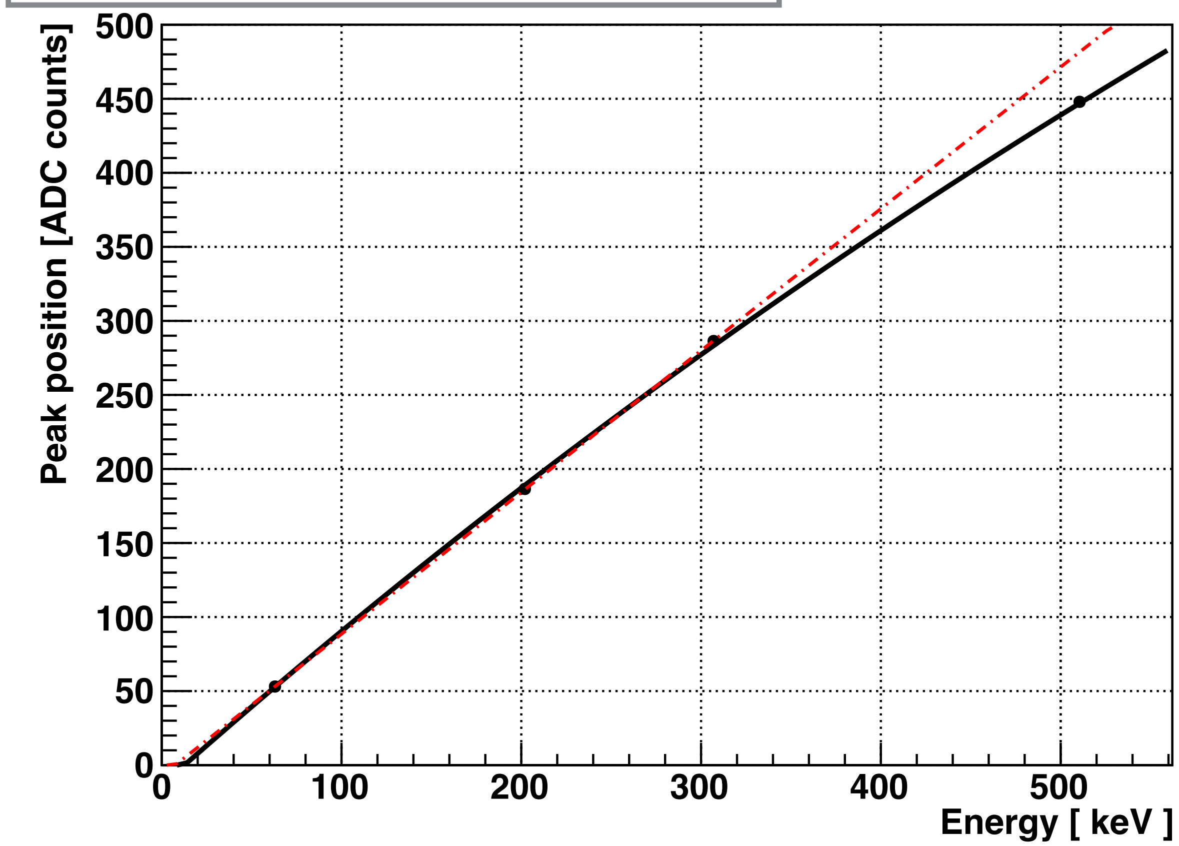

Energy resolution

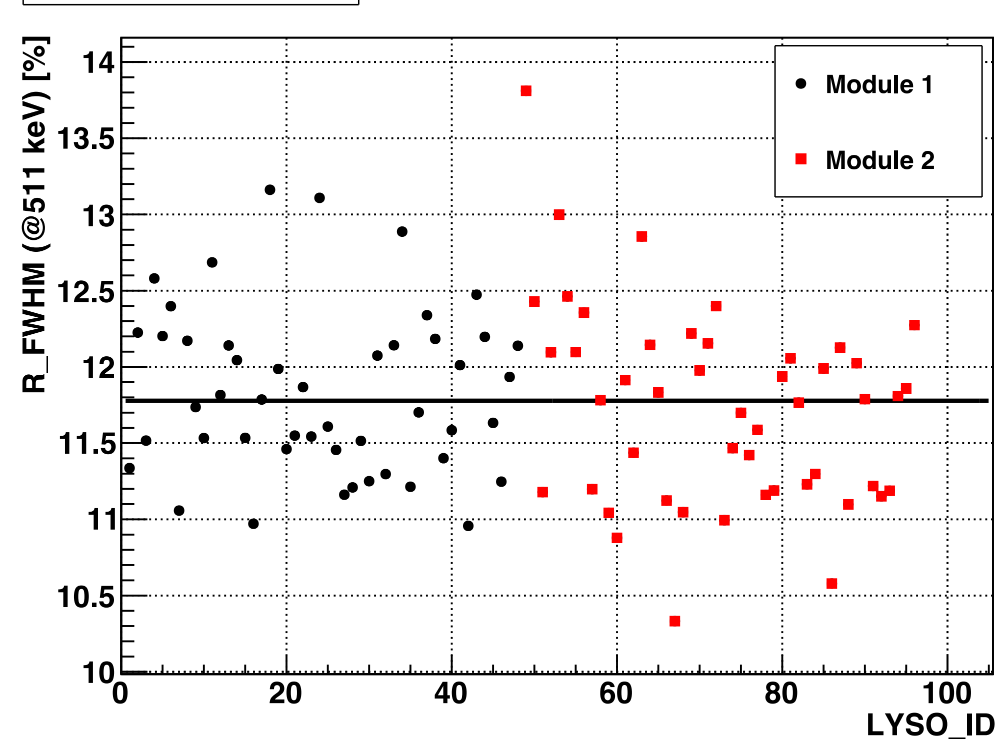

< ΔE_{FWHM} > ~11.8% @511 keV

(over two modules 96 LYSO crystals)

Axial resolution

Tagging crystal to scan the axial dimension in each module

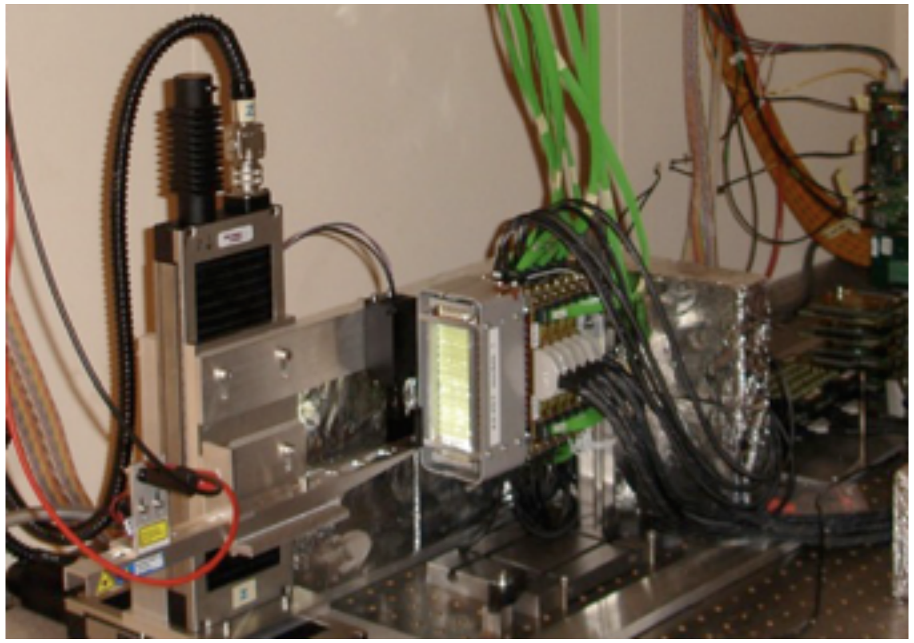

The two modules in coincidence

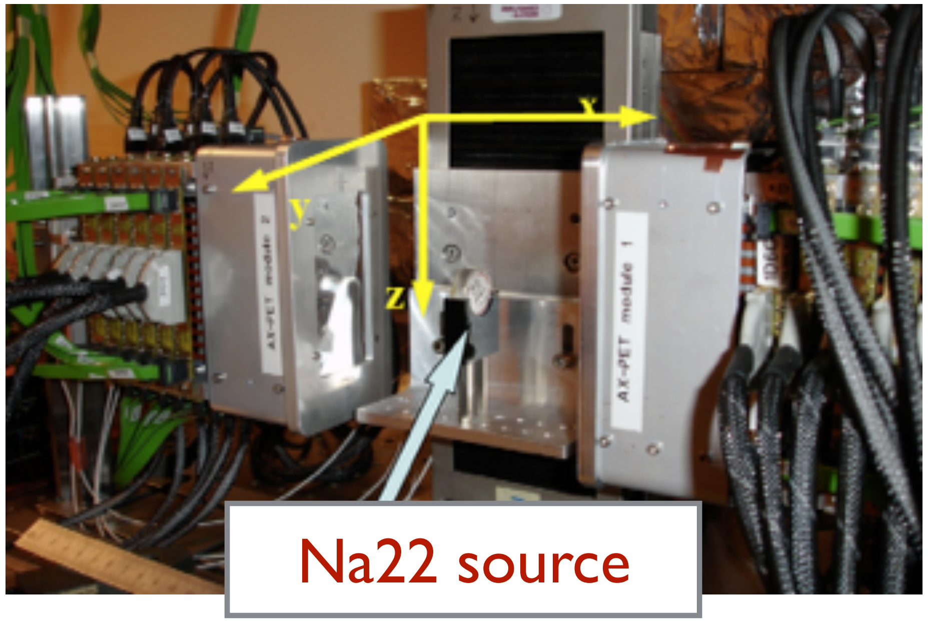

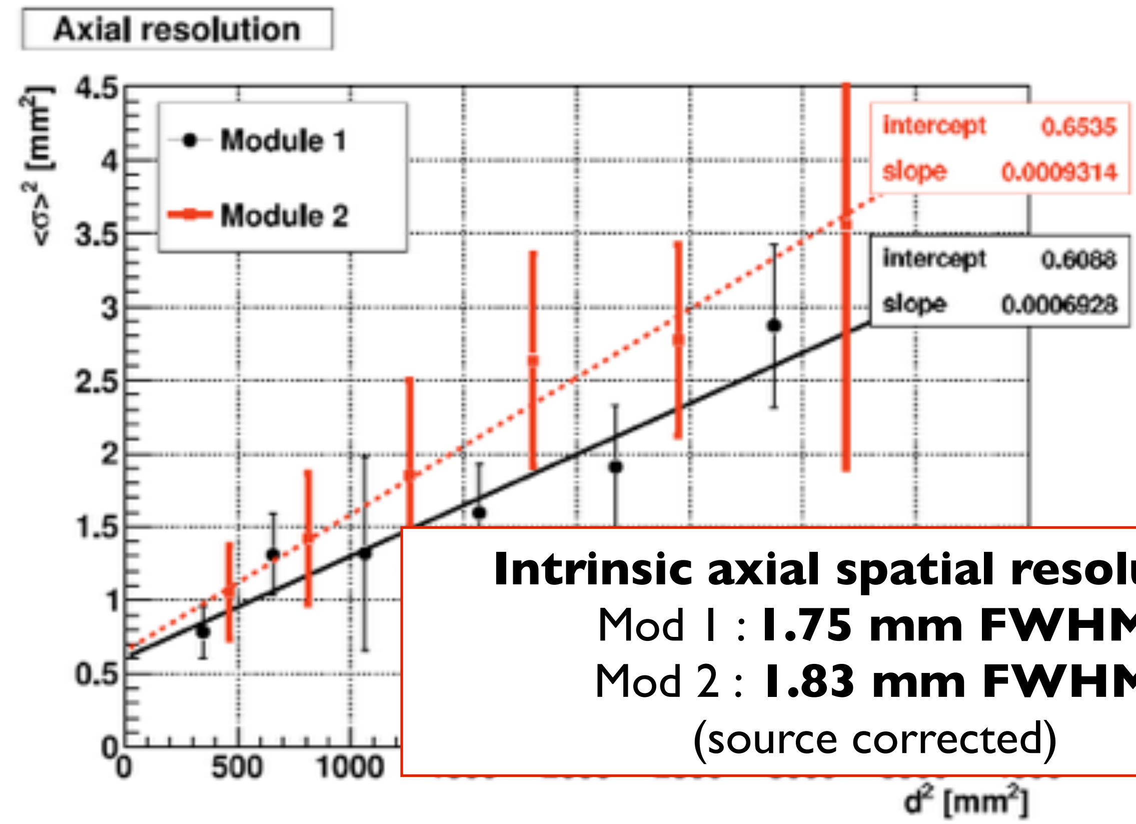

Intrinsic axial spatial resolution
Mod 1 : **1.75 mm FWHM**
Mod 2 : **1.83 mm FWHM**
(source corrected)

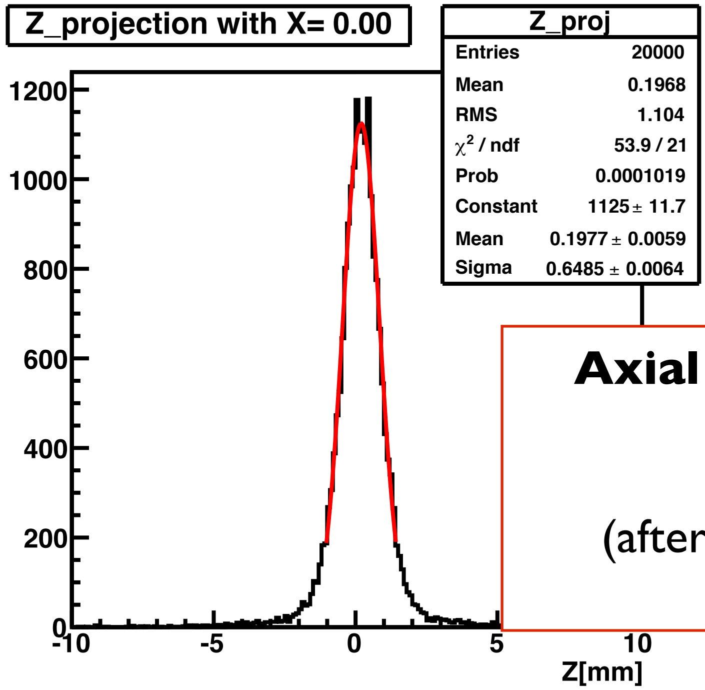

Axial resolution w/ LOR confocal reconstruction
1.35 mm FWHM
(after positron range and a-collinearity correction)

The proof-of-concept

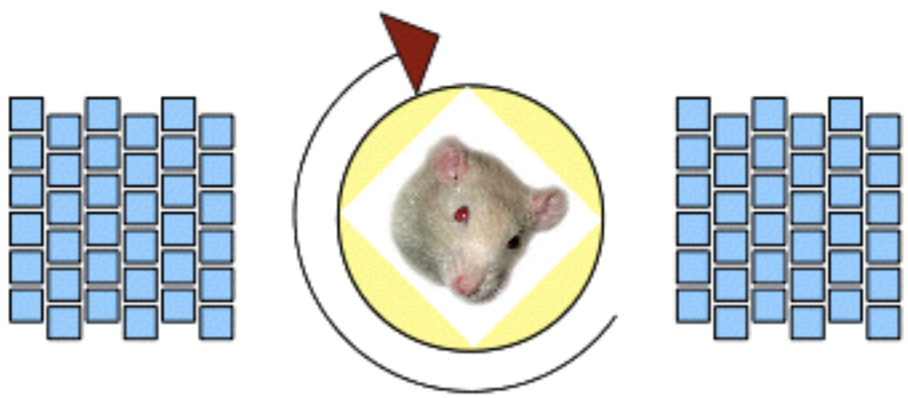

Face-to-face
θ = 0˚, 20˚, 40˚... 360˚ (18 steps)

Several measurement campaigns

1) global procedure test

Apr. 2010 ETH → Jul. 2010 AAA → Jul. 2011 AAA → Apr. 2012 ETH

Thin capillaries

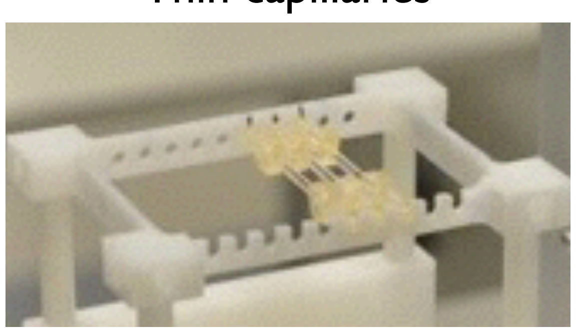

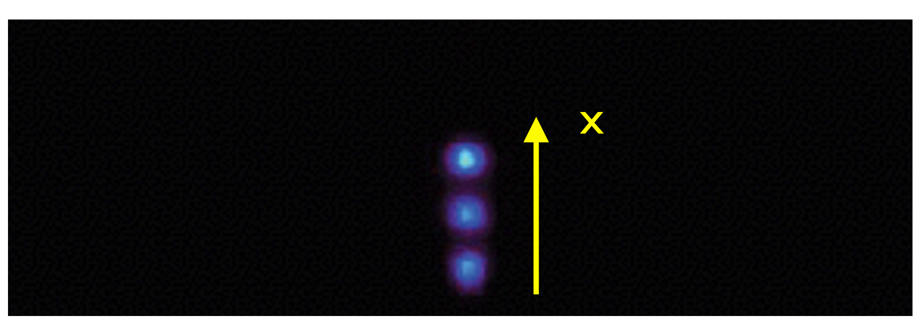

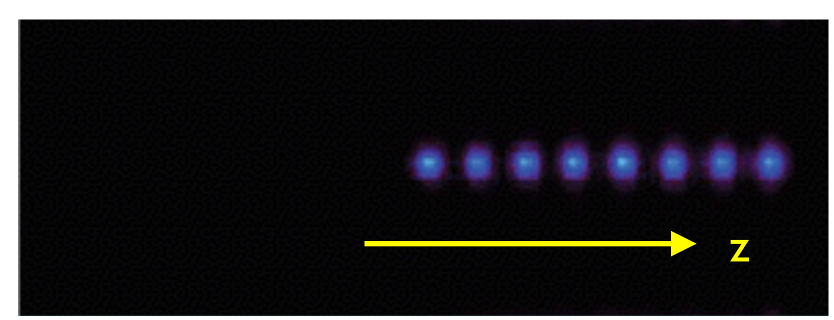

The proof-of-concept

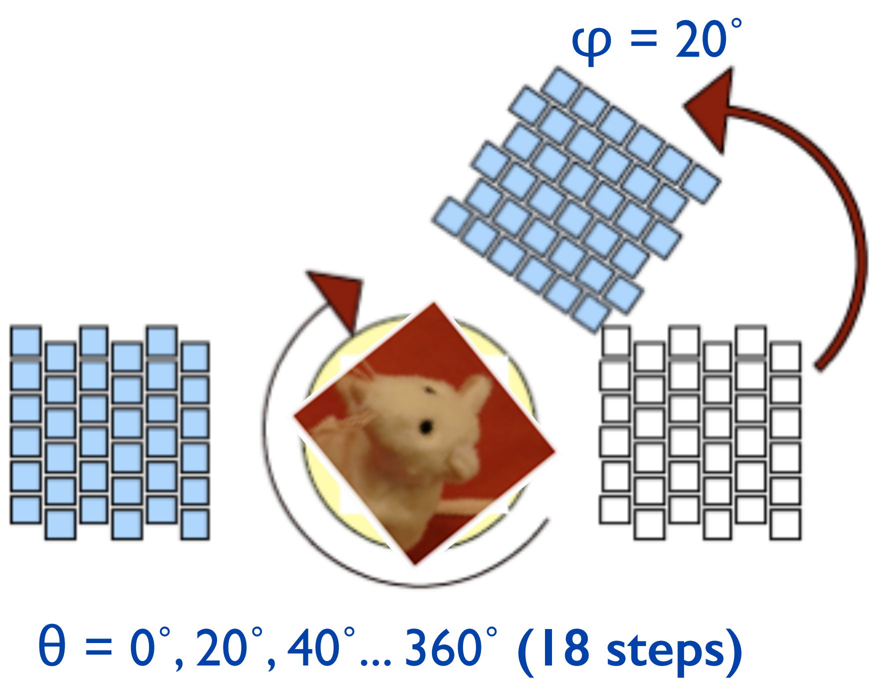

Several measurement campaigns

1) global procedure test

2) extended sources, extended FOV

Apr. 2010 ETH → Jul. 2010 AAA → Jul. 2011 AAA → Apr. 2012 ETH

Thin capillaries

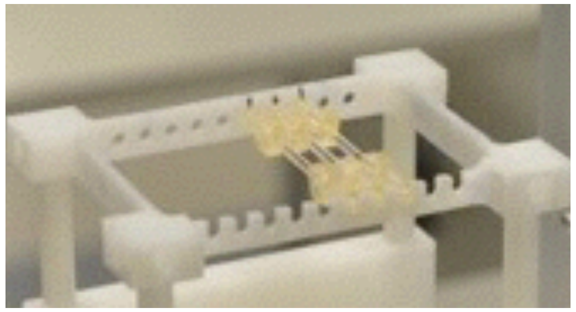

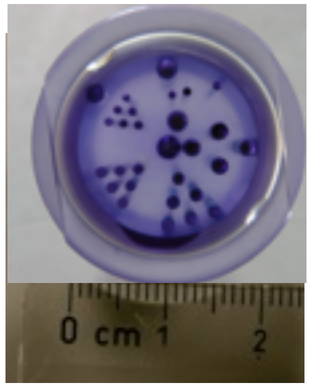

Micro-Derenzo

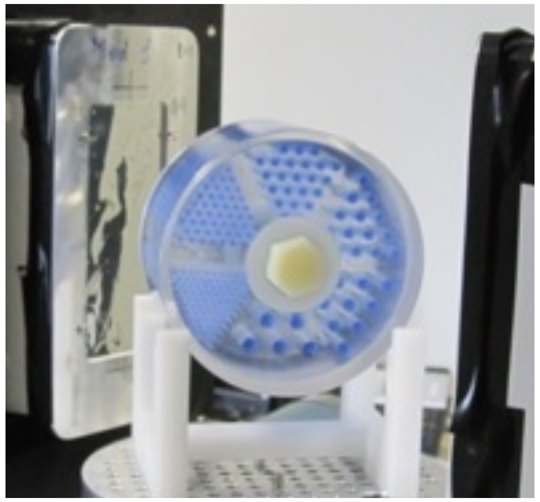

Mini-Deluxe

Homogeneous

NEMA

The proof-of-concept

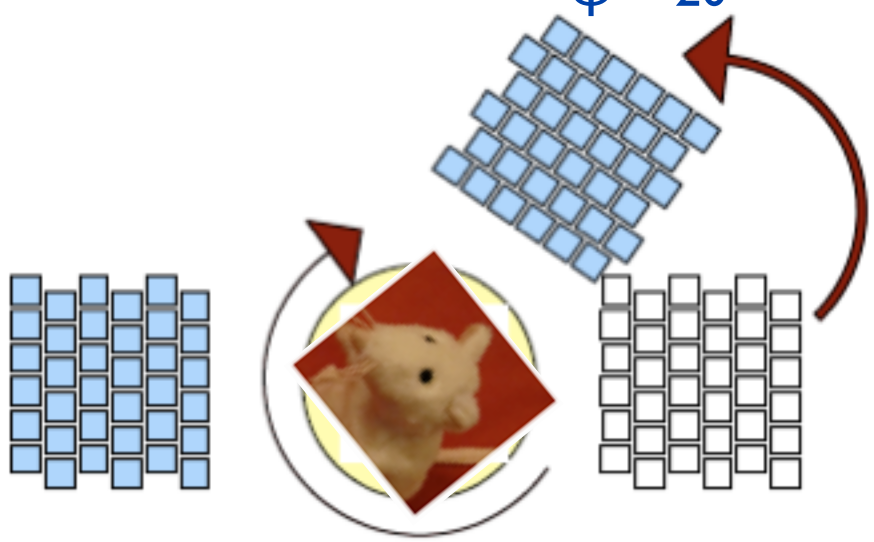

Several measurement campaigns

1) global procedure test
2) extended sources, extended FOV, fixed time per scan
3) Improved acquisition protocol: multiple scans per acquisition with adjusted acquisition time

Apr. 2010 ETH → Jul. 2010 AAA → Jul. 2011 AAA → Apr. 2012 ETH

Thin capillaries

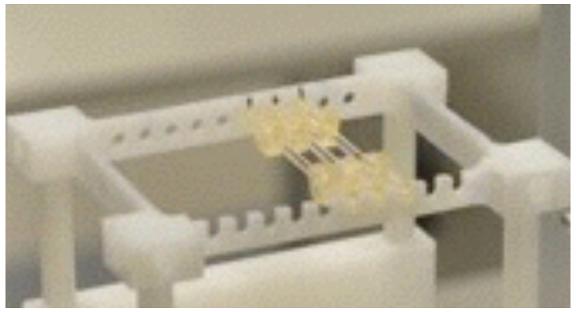

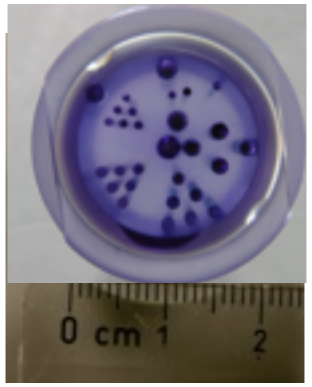

Micro-Derenzo

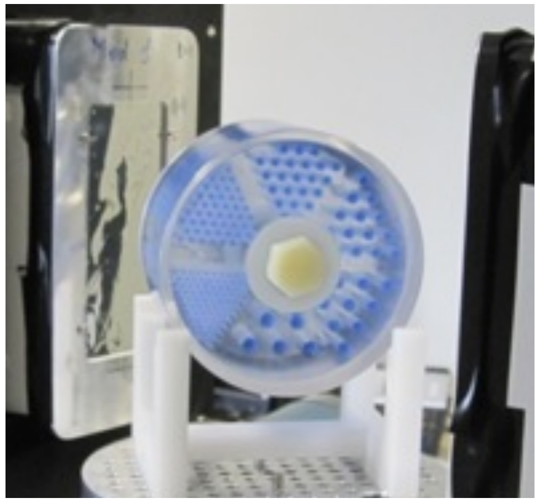

Mini-Deluxe

Homogeneous

NEMA

The proof-of-concept

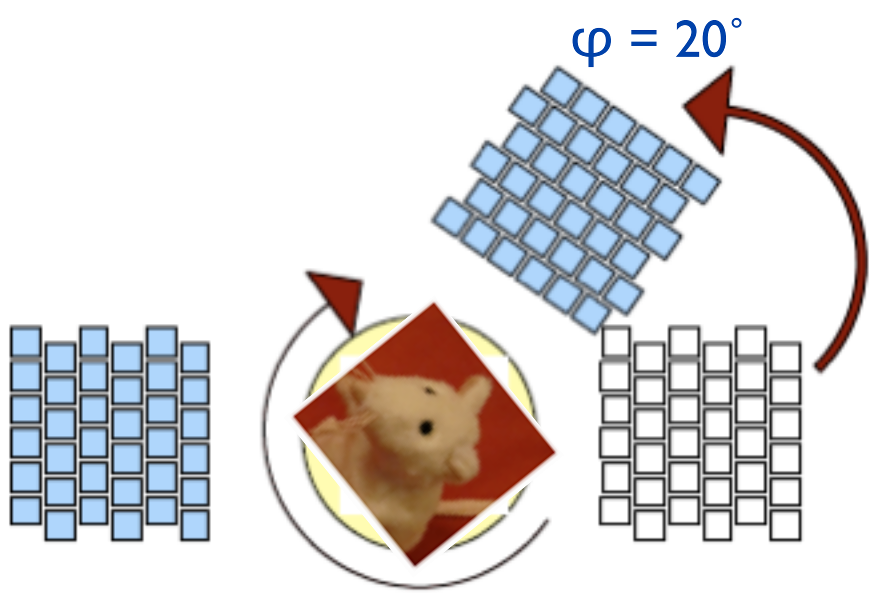

θ = 0°, 20°, 40°... 360° (18 steps)

Several measurement campaigns

1) global procedure test

2) extended sources, extended FOV, fixed time per scan

3) Improved acquisition protocol: multiple scans per acquisition with adjusted acquisition time

4) Imaging small animals

Apr. 2010 ETH → **Jul. 2010 AAA** → **Jul. 2011 AAA** → **Apr. 2012 ETH**

Thin capillaries

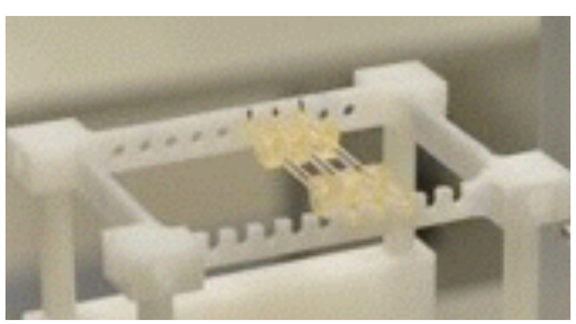

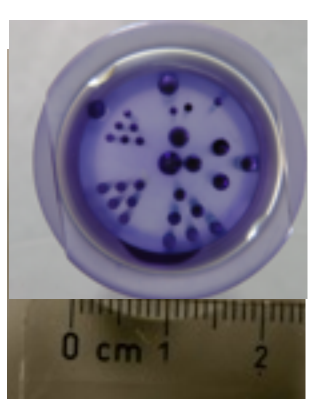

Micro-Derenzo

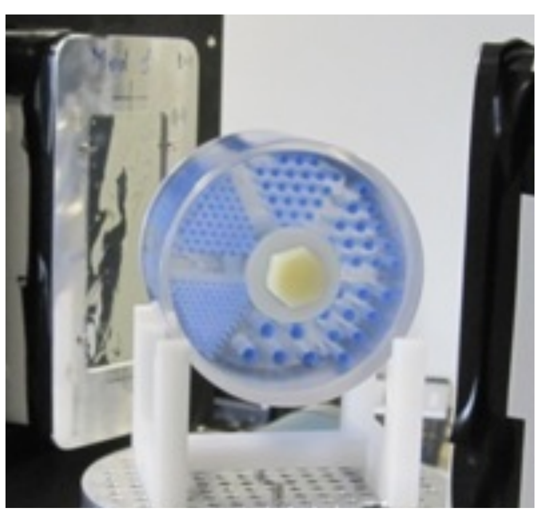

Mini-Deluxe

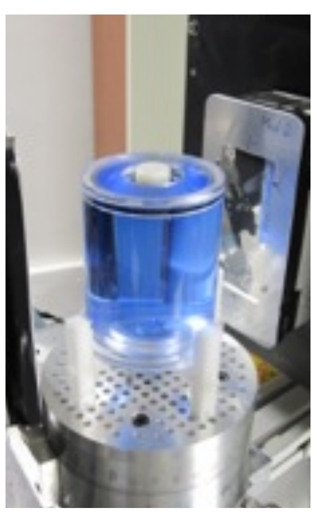

Homogeneous

NEMA

Rat and Mouse

The proof-of-concept

63 mm

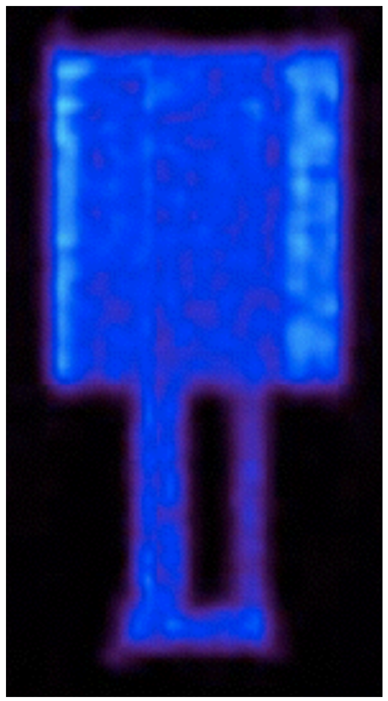

1 mm rod reconstructed with 1.6 mm FWHM

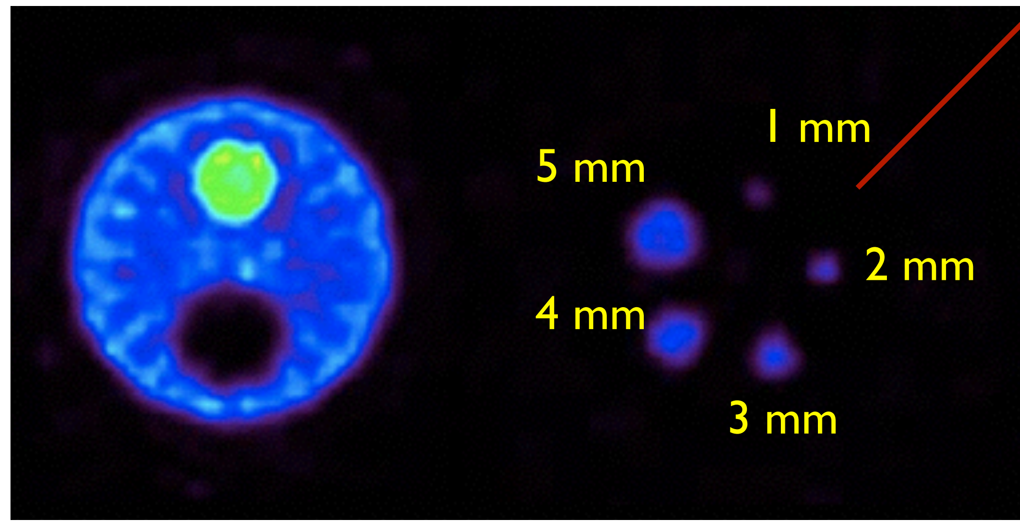

- Reconstruction: LOR-Histogram +off-line SM
- 4.20×10^8 LORs
- Voxel size: 1x1x1 mm^3
- No corrections
- 100 iterations

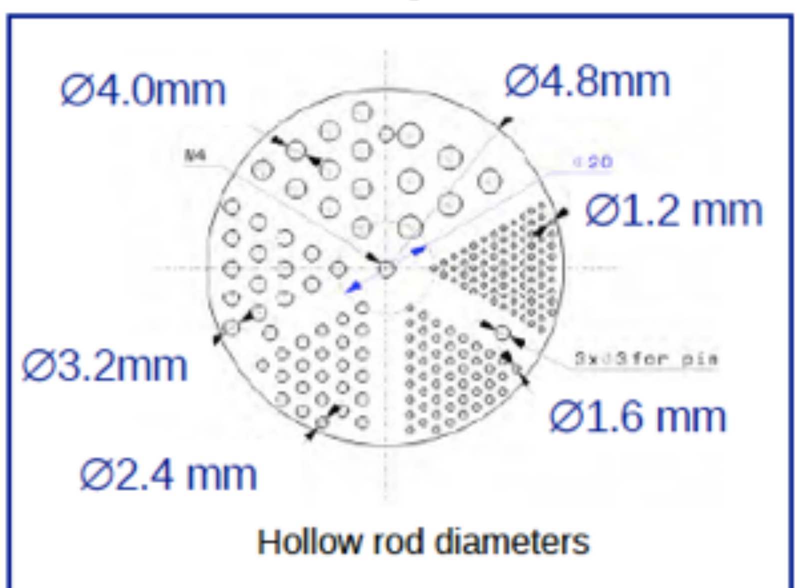

AAA 2011

Rods parallel to z axis

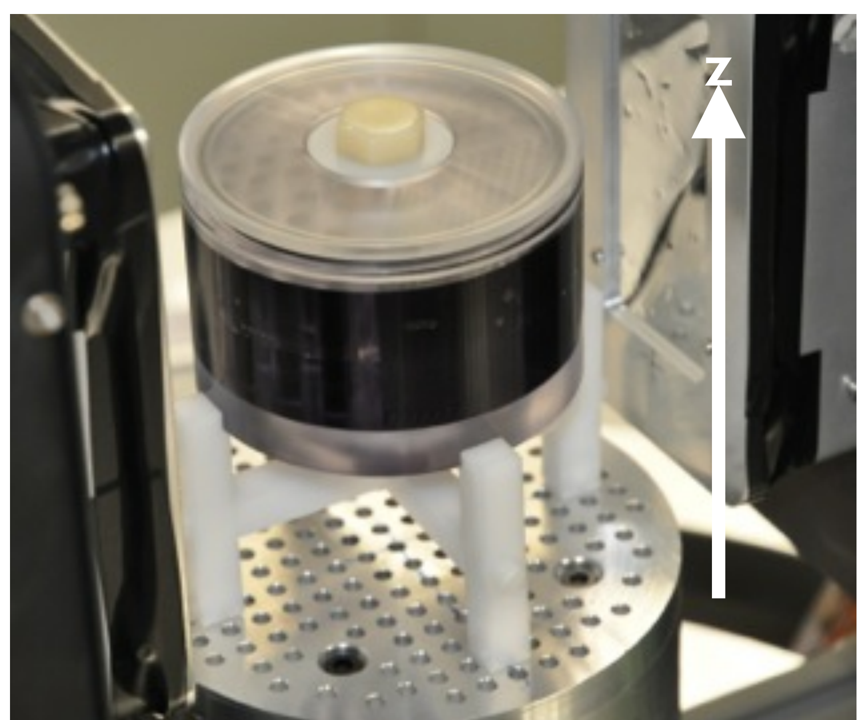

Rods perpendicular to z axis

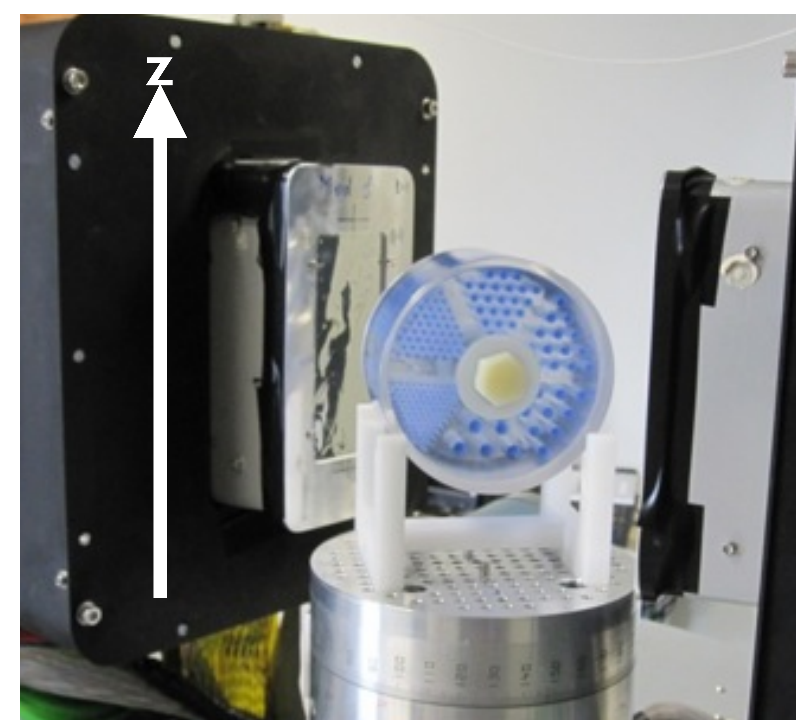

The proof-of-concept

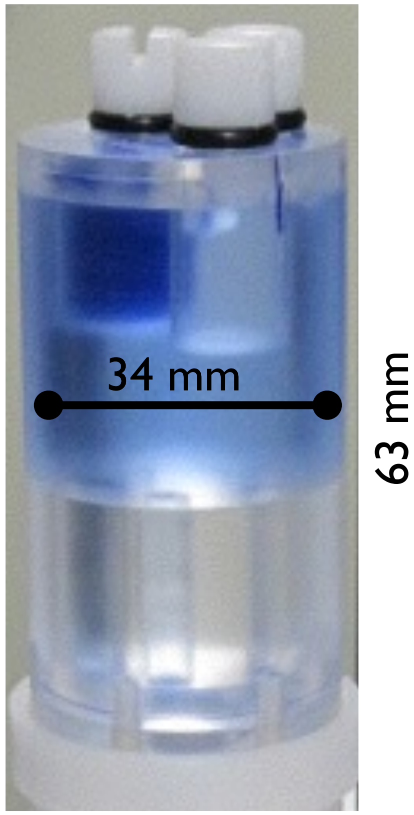

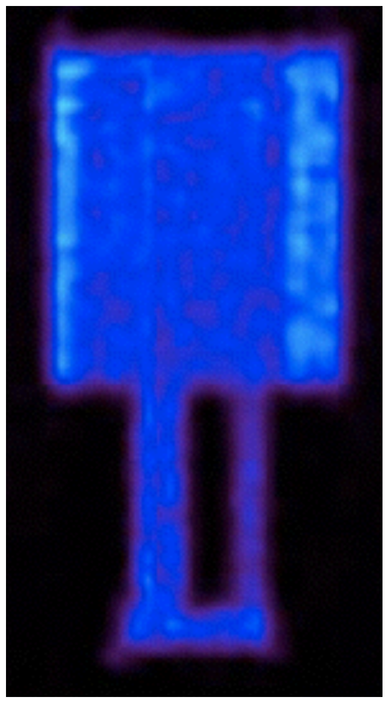

1 mm rod reconstructed with 1.6 mm FWHM

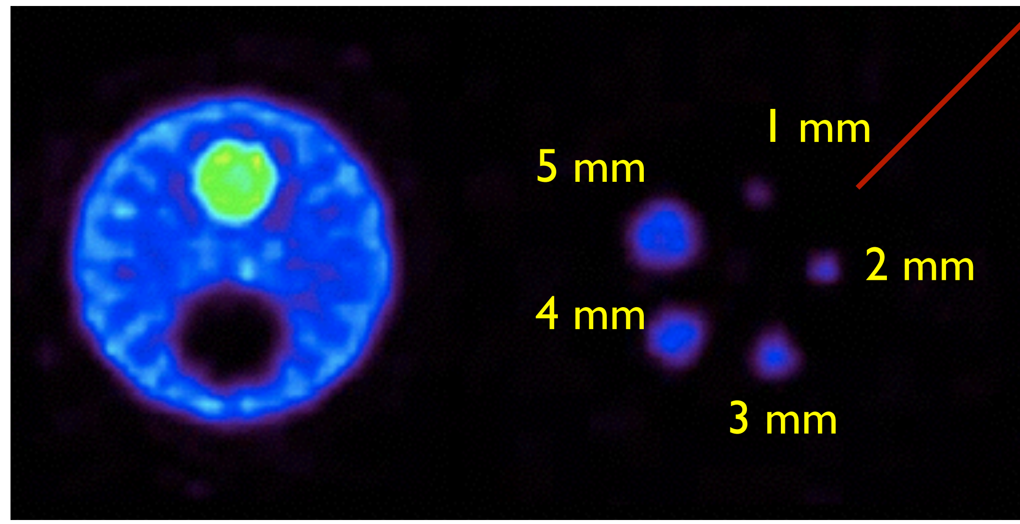

- Reconstruction: LOR-Histogram +off-line SM
- 4.20 × 10^8 LORs
- Voxel size: 1x1x1 mm^3
- No corrections
- 100 iterations

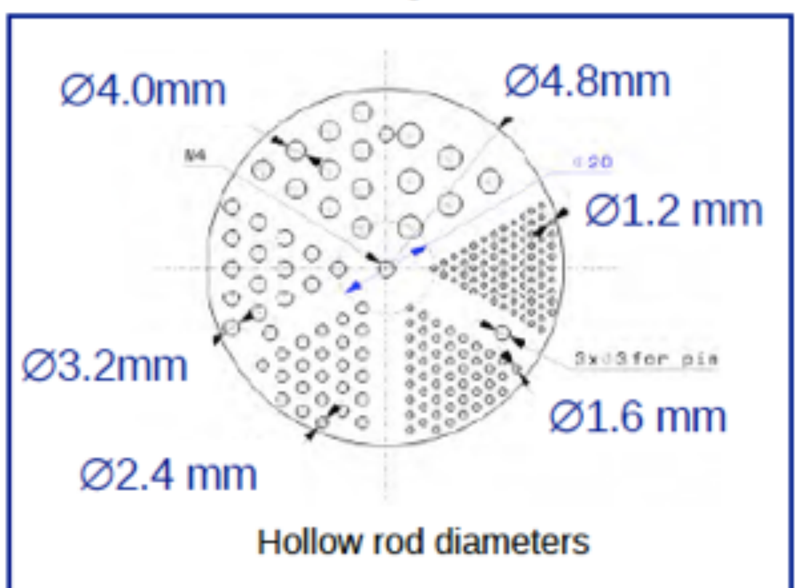

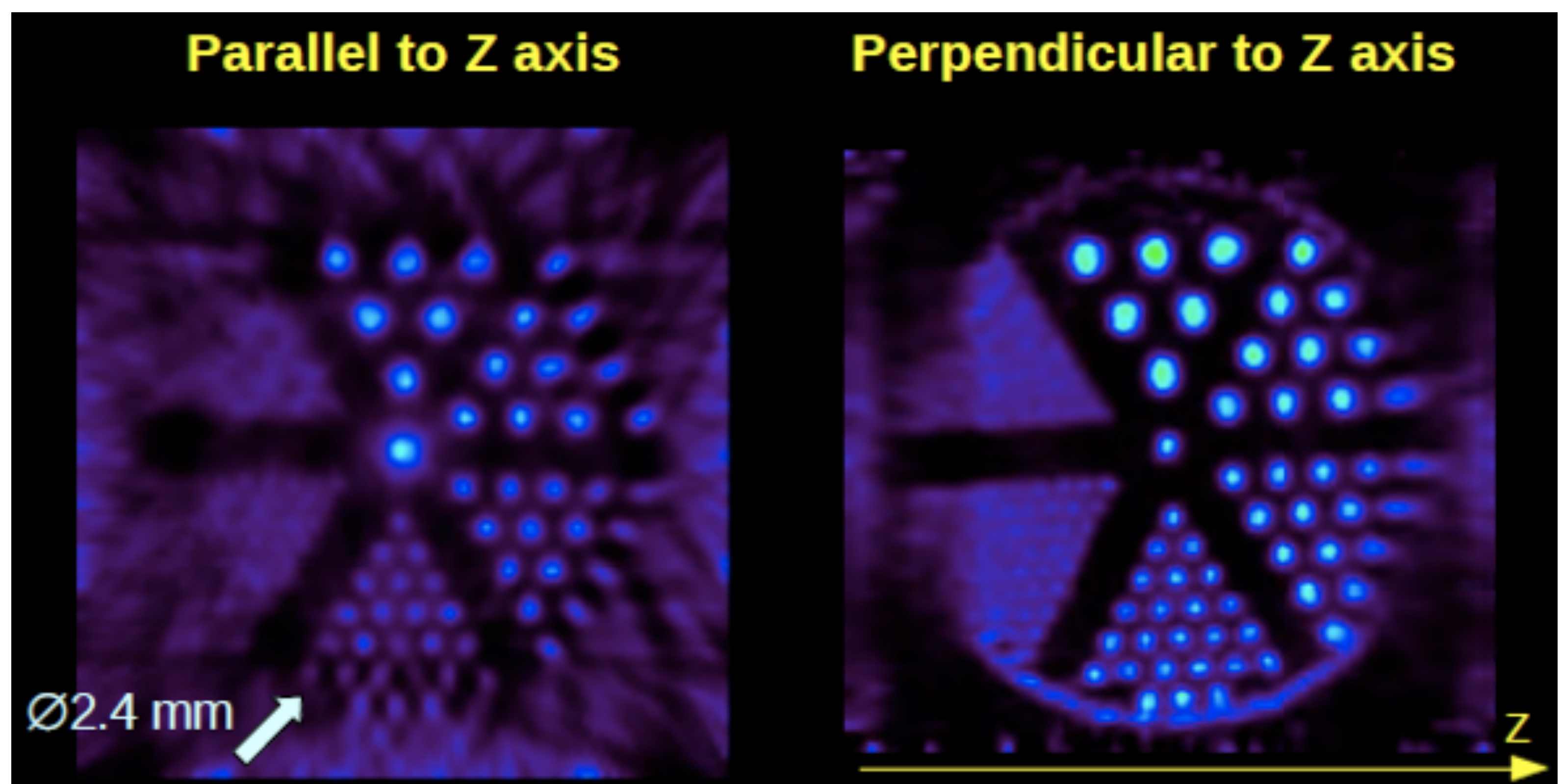

AAA 2011

Software developments

Challenges (just some of them..)

- Two coordinates with different readouts: continuous z and discrete x-y.
  - **List-mode data** allows to preserve spatial resolution, no binning is required.

- Prototype in continuos evolution: different acquisition protocols, FOV varies.
  - **System Response Matrix** calculation required in ML-EM reconstruction: off-line (more accurate, computationally consuming) and on-the-fly (less accurate but better deals with prototype evolution).

- Novel device with features that require dedicated reconstruction approaches.
  - **Inter-Crystal Scatter events:** it has the potential to enhance sensitivity but resolution shall be preserved.

- Monte Carlo support is required to support the prototype predictions and developments, test reconstruction SW, bring some light on measurements understanding.
  - Common tool such as GATE can't model such a complex system, **dedicated Monte Carlo** model is required.

Software developments: ICS inclusion

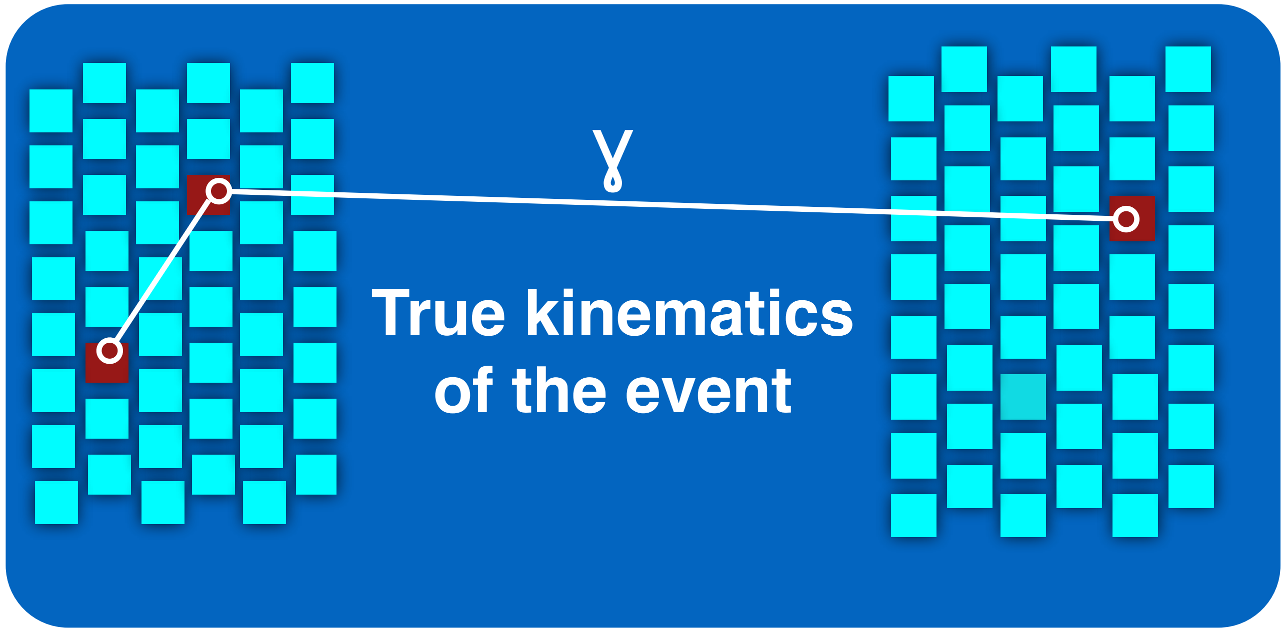

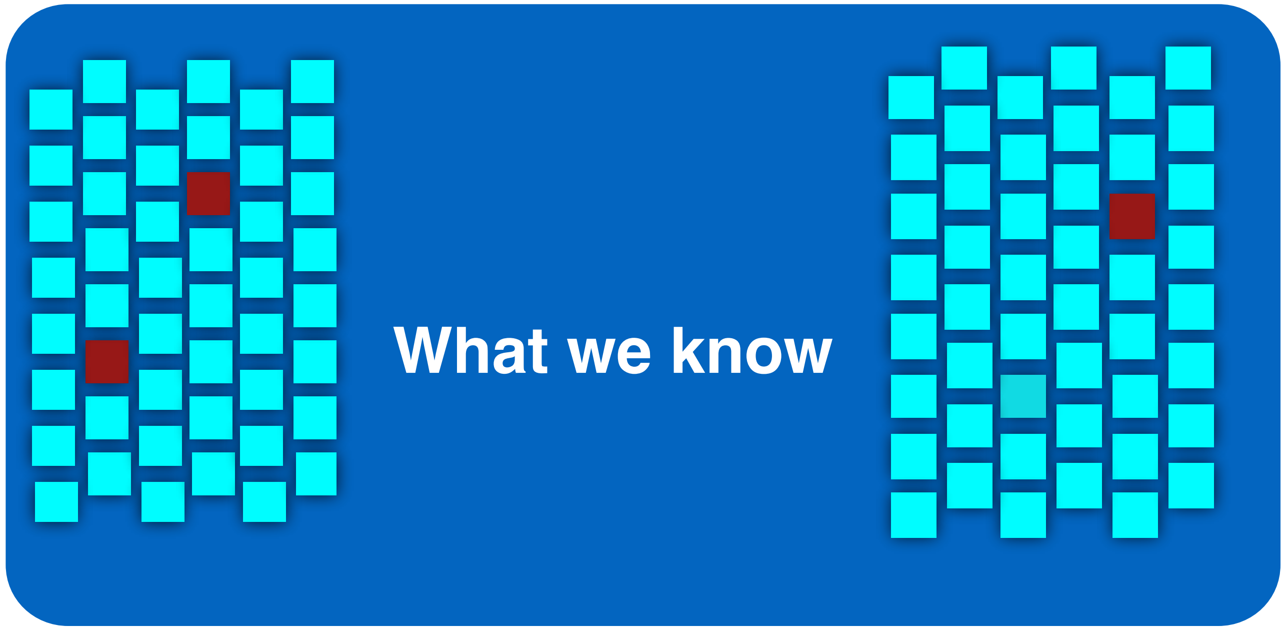

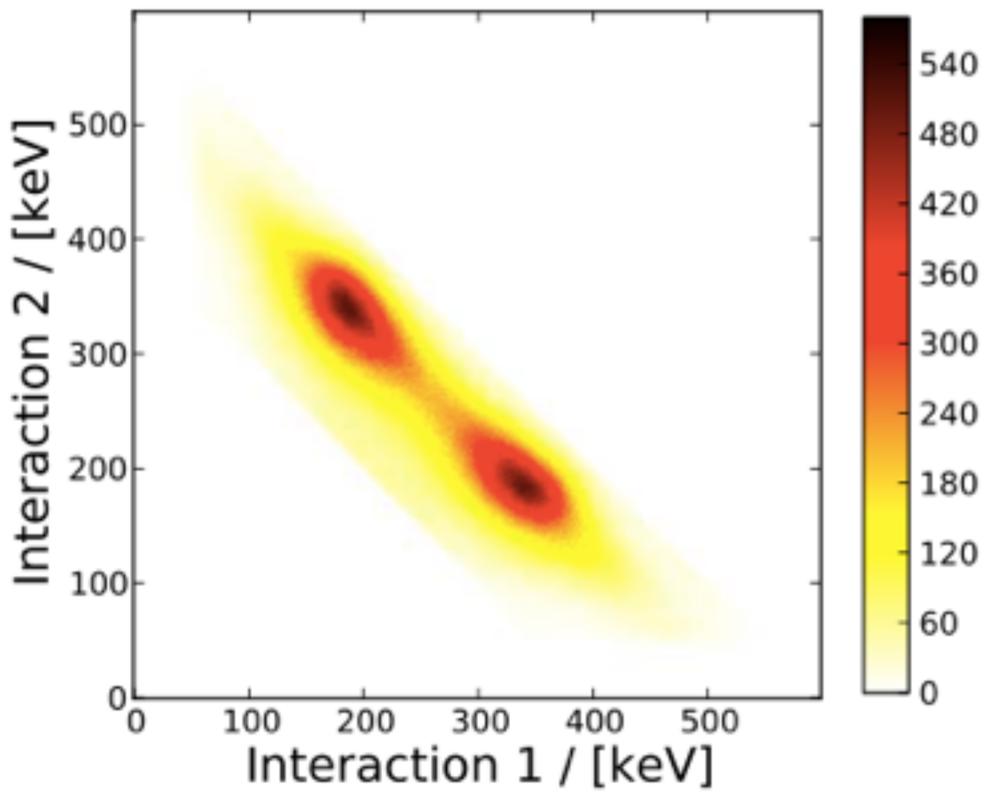

- The gamma undergoes multiple Compton interactions within the module (~30%)
- We can't access the true kinematics of the event.
- **How to deal with it at reconstruction level?**

Software developments: ICS Inclusion

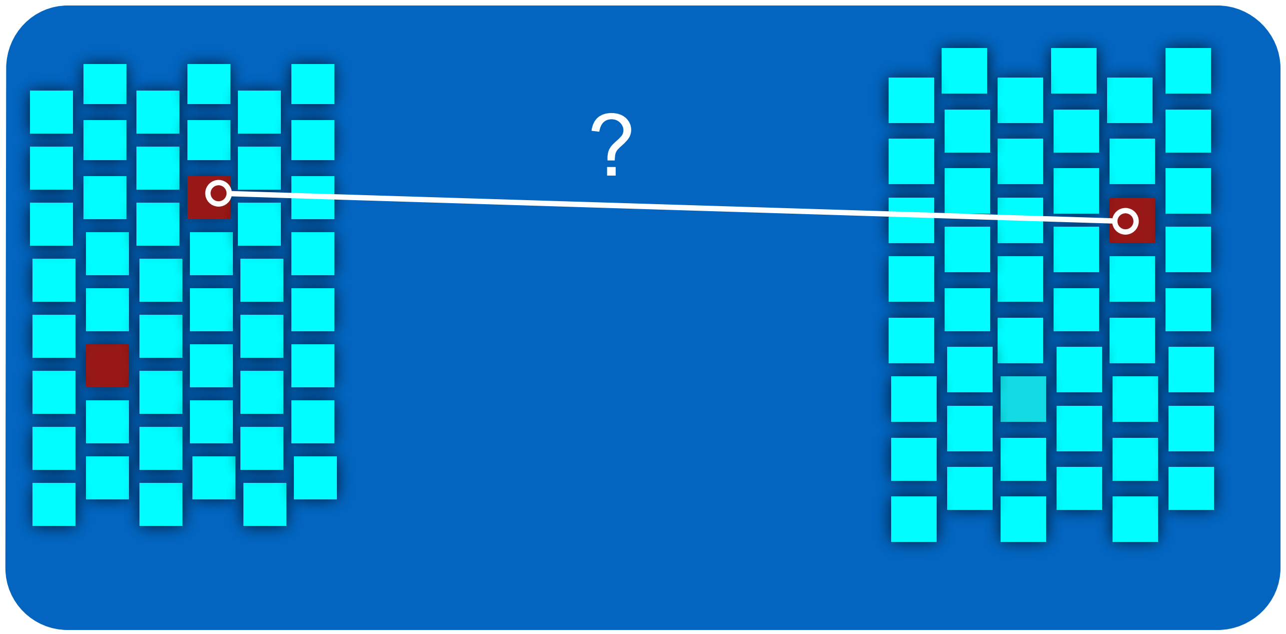

Conventional approach

- Selection: selecting one of the two LORs by probability criteria
- low identification success rate (~70% so far with NN)

$$a_1, a_2: \quad \begin{cases} a = a_1 \text{ if } w_1 > w_2 \\ a = a_2 \text{ if } w_2 > w_1 \end{cases}$$

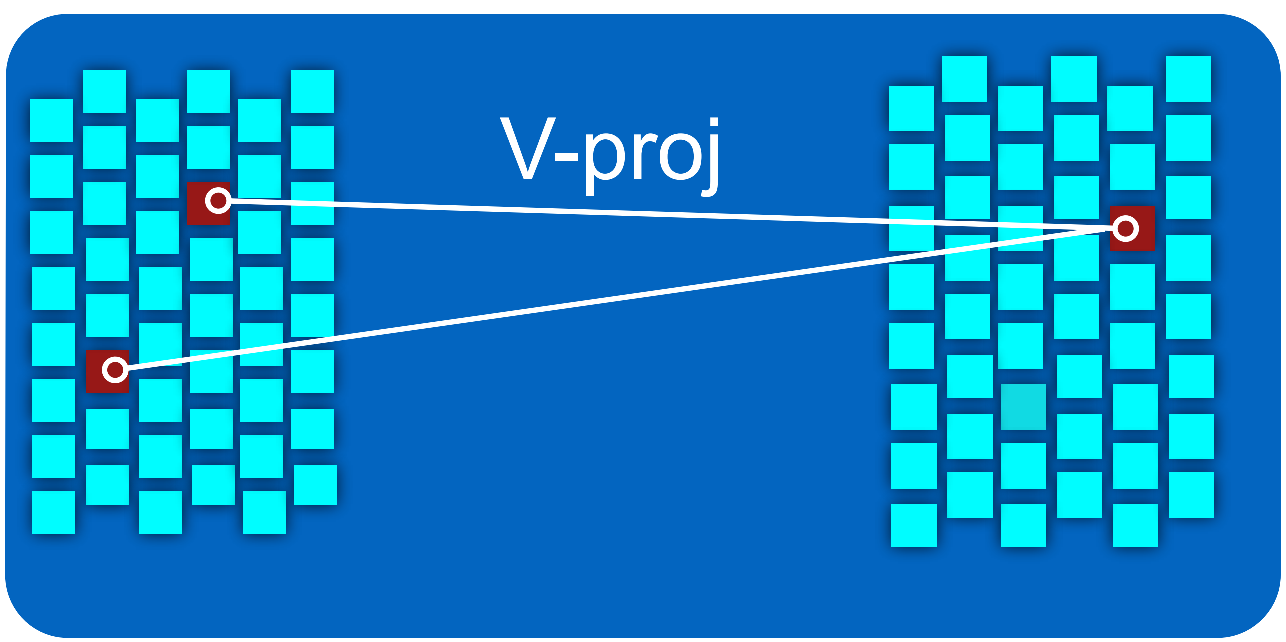

Proposed approach

- Reconstruct both LORs that is preserving the full probability function associated to the V-shape.

$$a_1, a_2: \quad a = w_1 a_1 + w_2 a_2$$

Software developments: ICS Inclusion

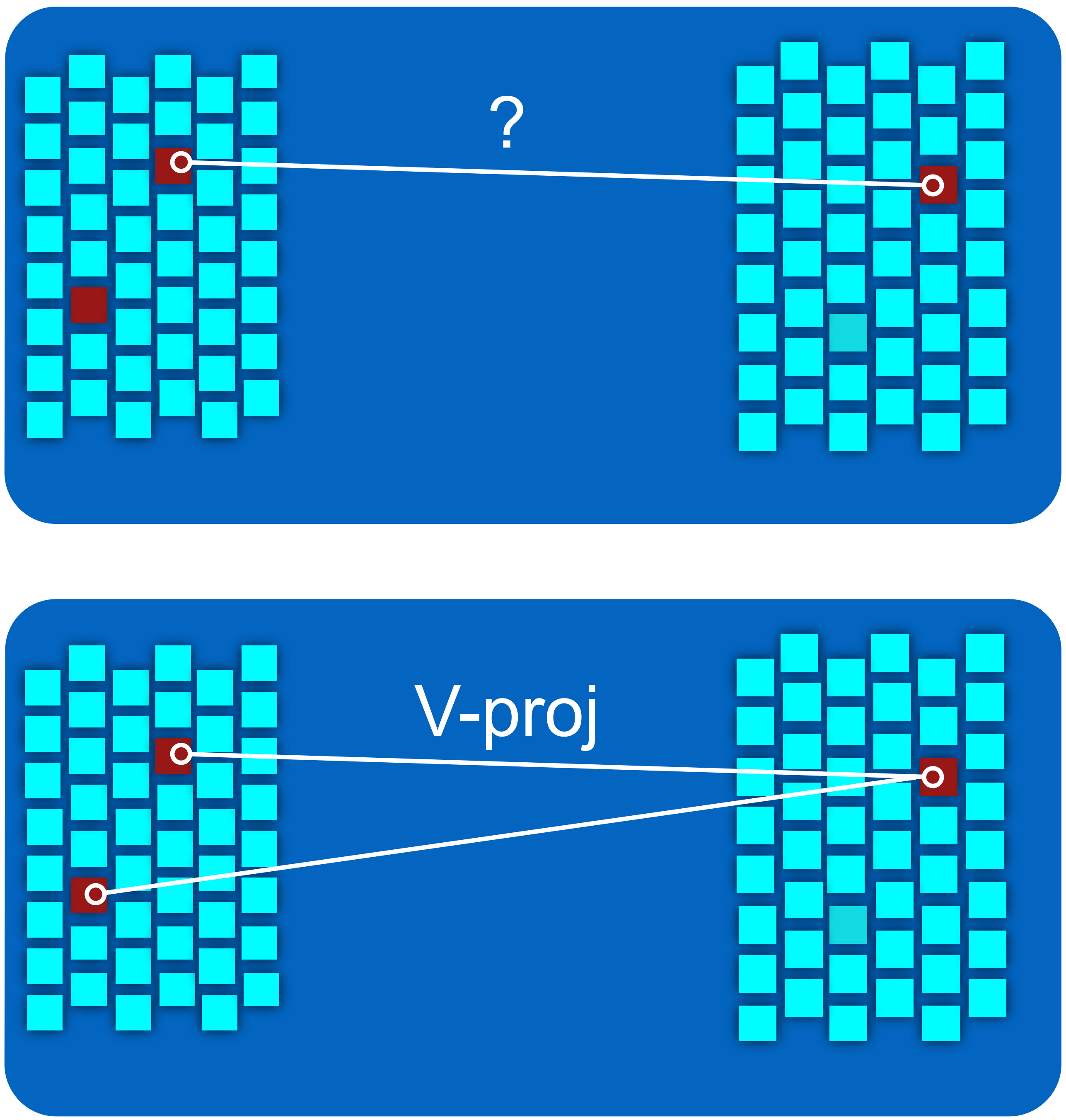

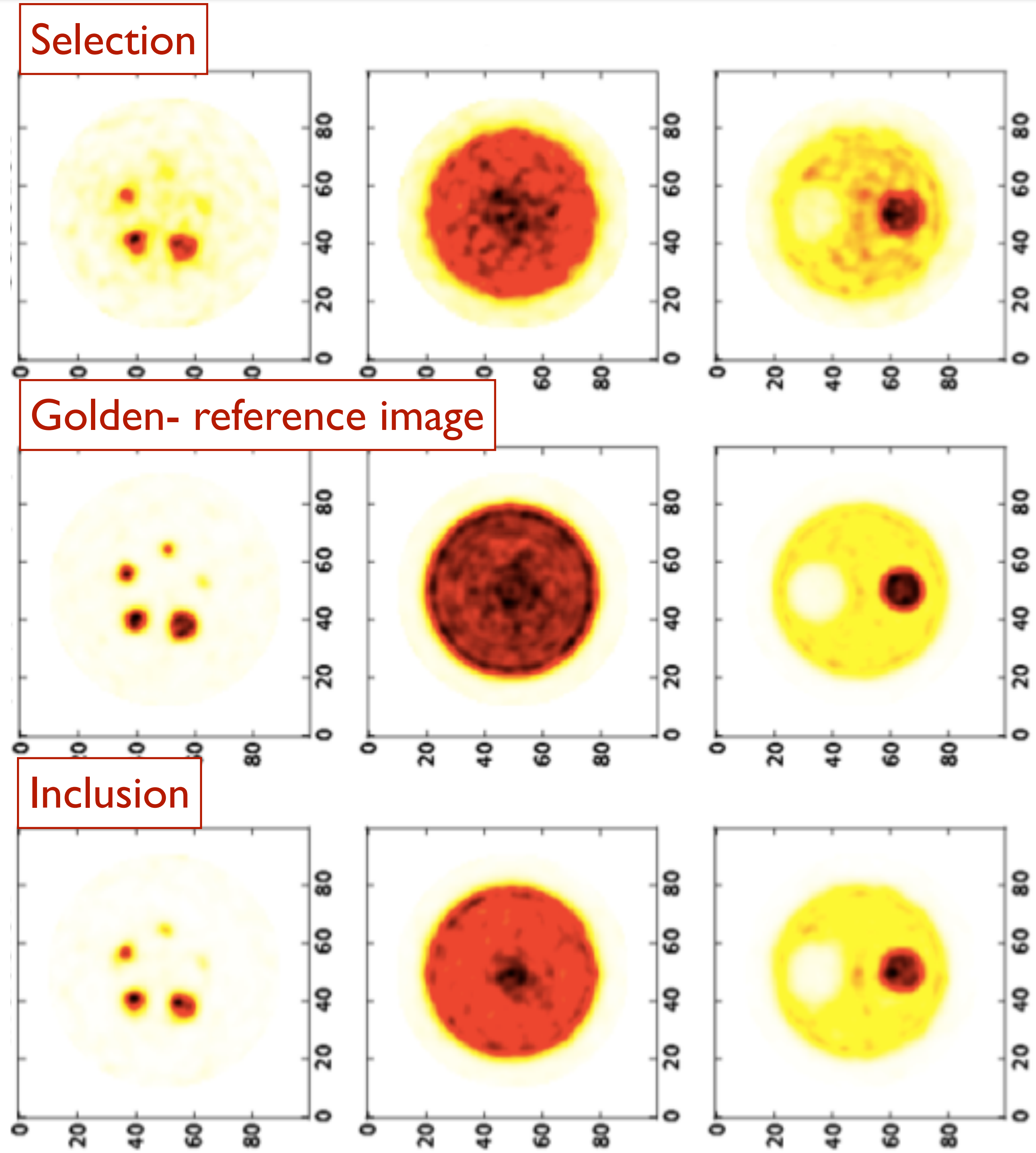

AAA 2011

J.E. Gillam et al, PMB 59(2014)

Software developments: ICS Inclusion

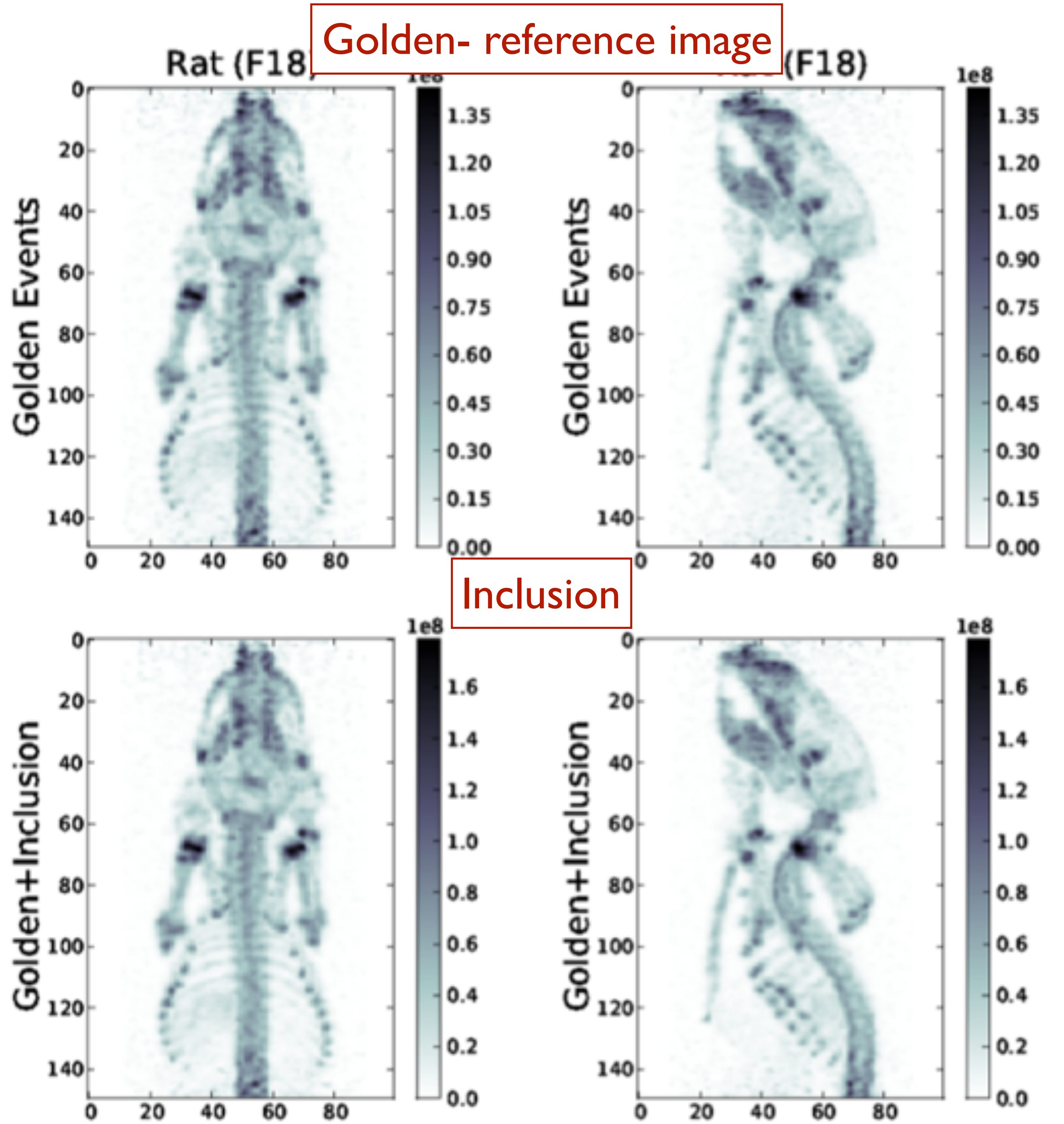

General considerations

- Sensitivity increases in all imaged subjects.
- SNR improves but not as much as sensitivity.
- Increase in noisy counts in cold regions (see NEMA) is mitigated by the inclusion approach than other conventional ICS treatments.

ETH 2012

J.E. Gillam et al, PMB 59(2014)

Software developments: Monte Carlo

Dedicated Monte Carlo model based on GATE classes.

- Geometry of the detector (staggering, layered, etc.)
- WLS response model: it has to be computationally efficient therefore an analytical model of the signal on the strips is tuned on experimental data from dedicated experimental set-ups.
- Intrinsic radioactivity
- Dedicated coincidence sorter: WLS channels shall be treated as well, hybrid dead-time model, etc.

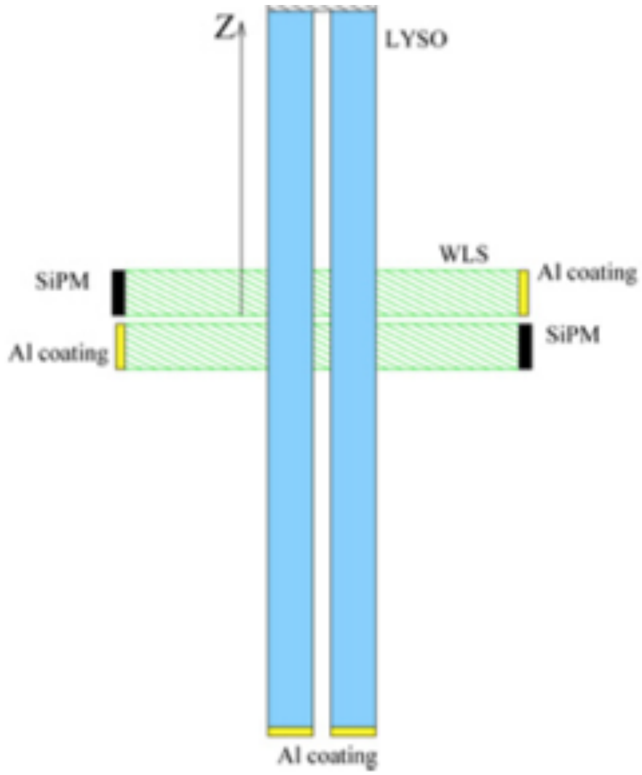

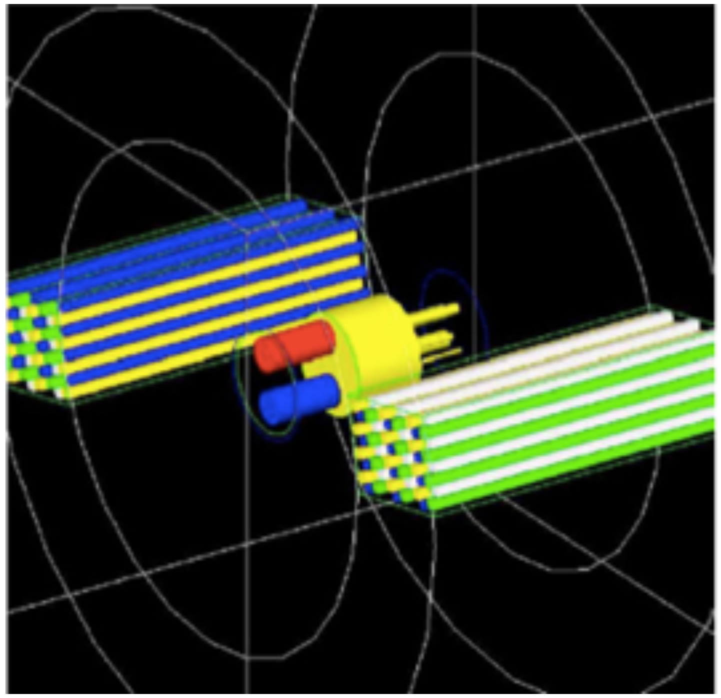

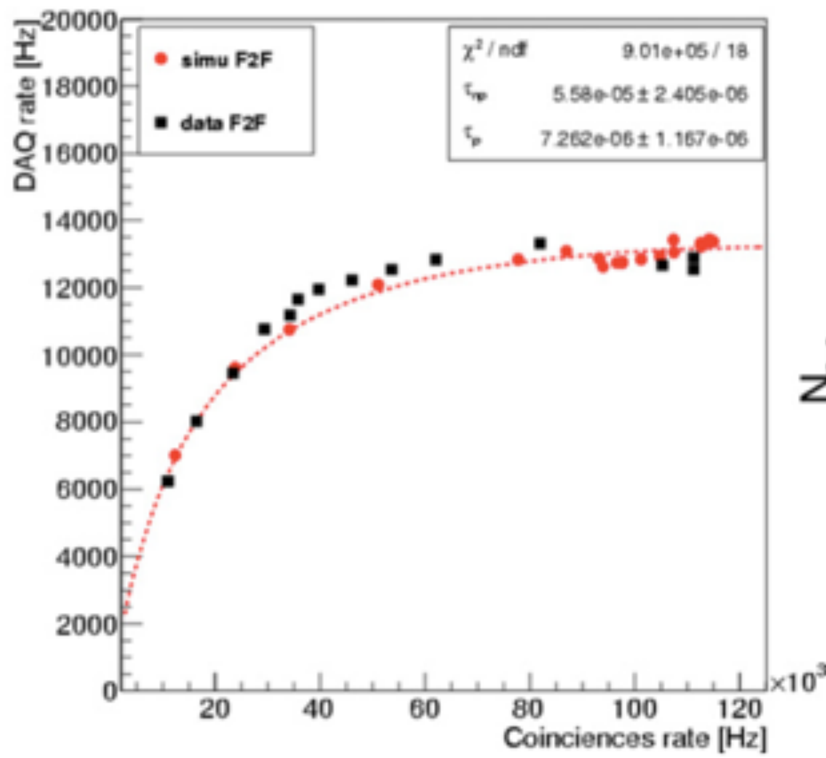

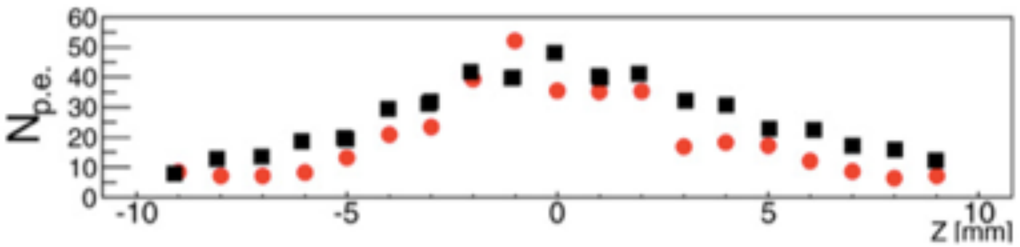

P. Solevi et al, PMB 58(2013)

AX-PET for brain imaging

- AX-PET was at the very beginning conceived for Brain Imaging (3x3 mm^2 crystal cross section, high axial resolution, etc).

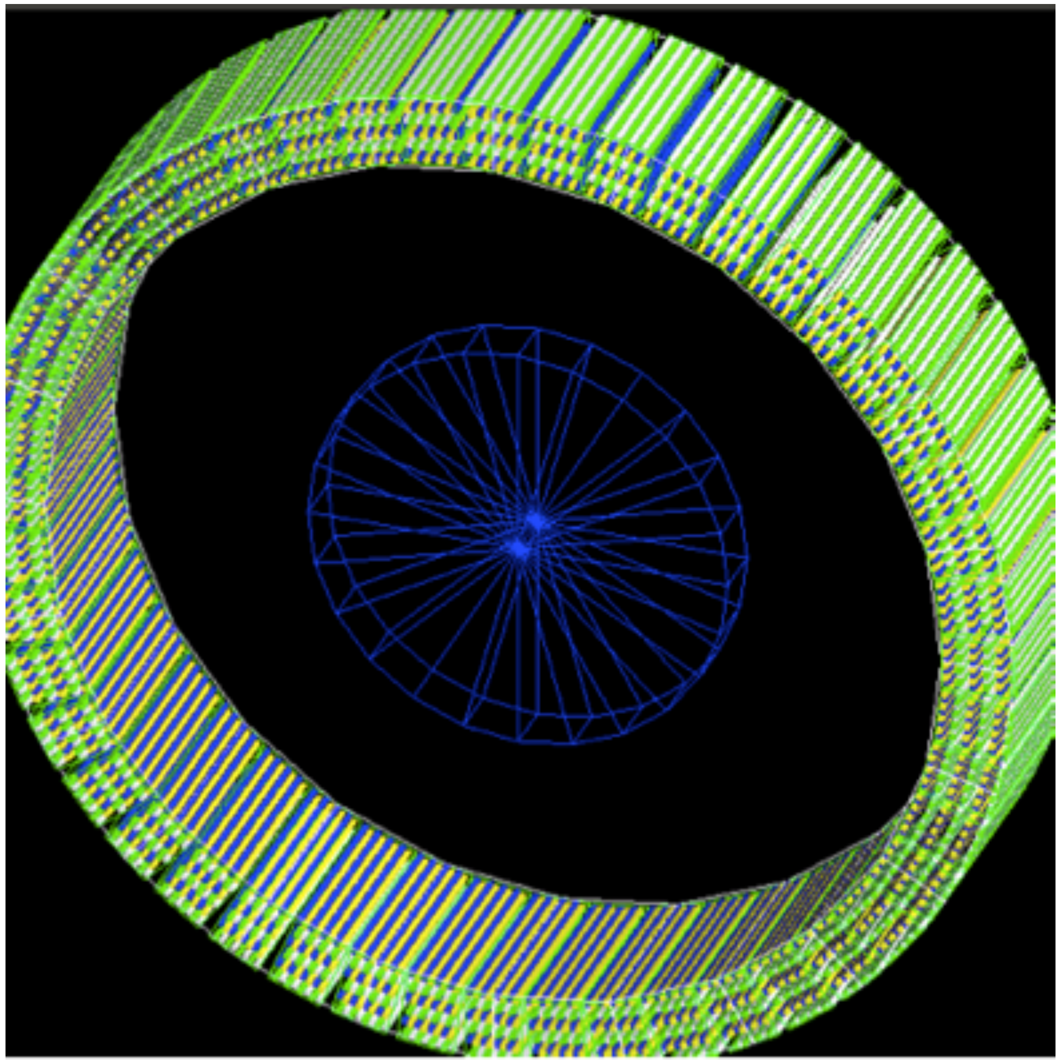

Demonstrator design

- 48 modules arranged over a ring of 468 mm diameter.
- Electronics performance improved (within a realistic technological horizon):
  - 75 ns integration time window (pile-up)
  - [400,650] keV @ module
  - 5 ns coincidence window
  - Improved dead-time at DAQ level

Can we do better?

AX-PET for brain imaging

- AX-PET was at the very beginning conceived for Brain Imaging (3x3 mm^2 crystal cross section, high axial resolution, etc).

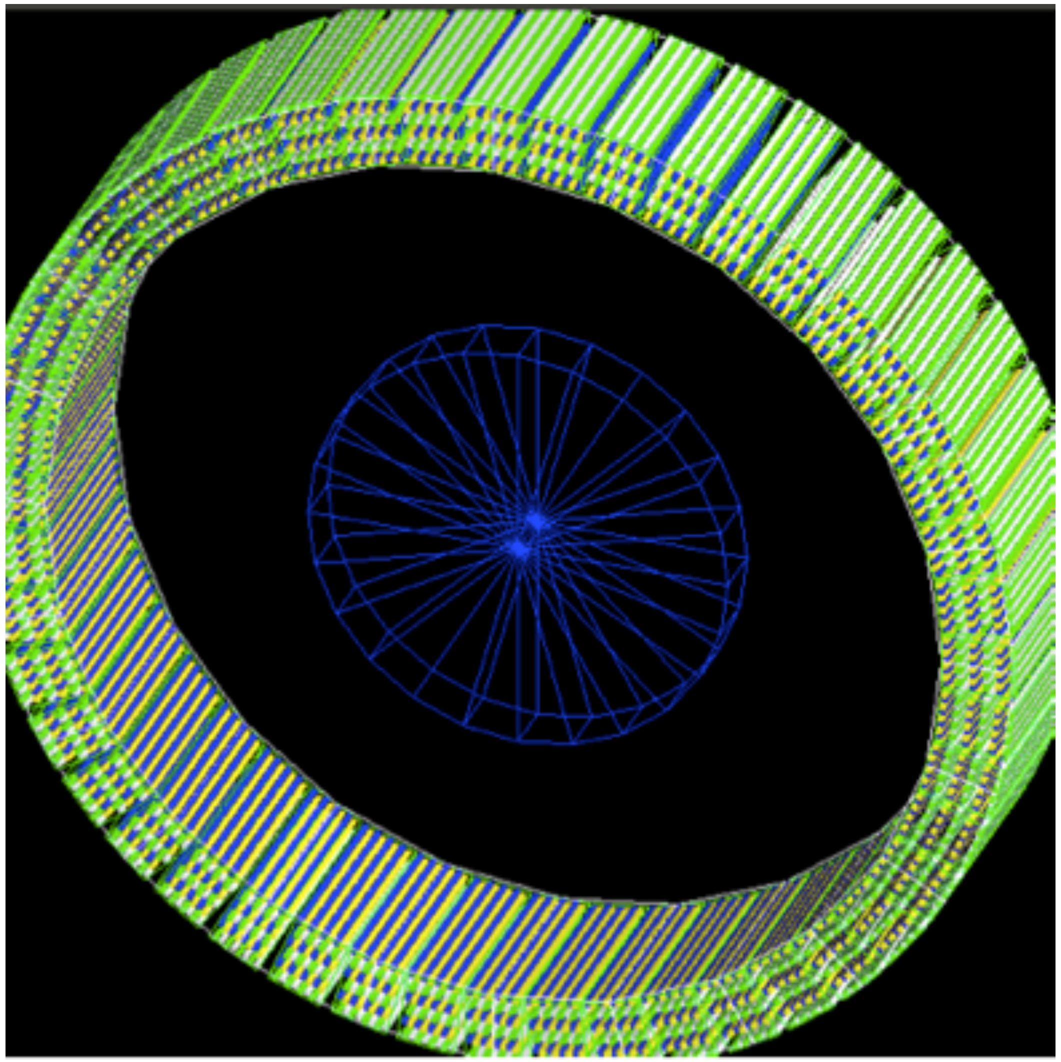

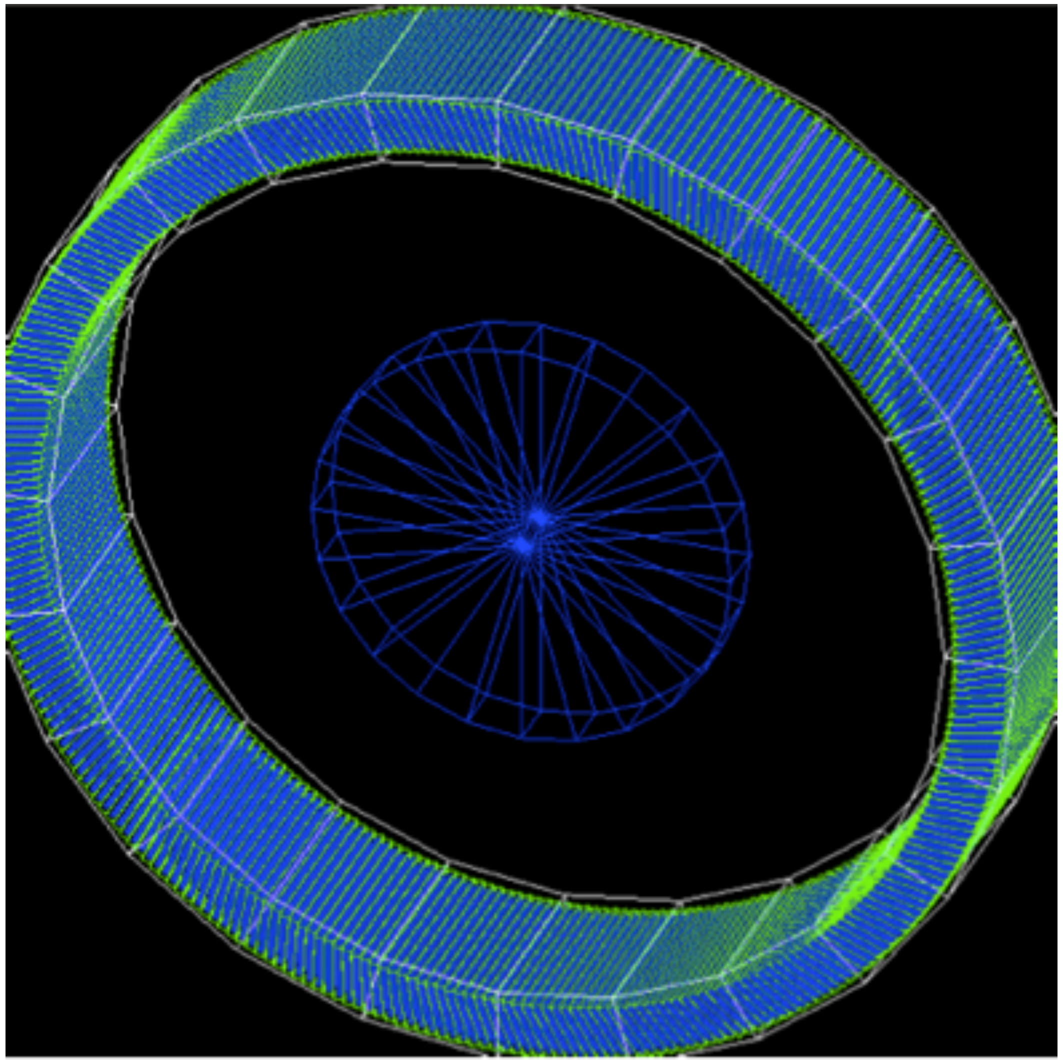

AX-PET for brain imaging

- AX-PET was at the very beginning conceived for Brain Imaging (3x3 mm^2 crystal cross section, high axial resolution, etc).

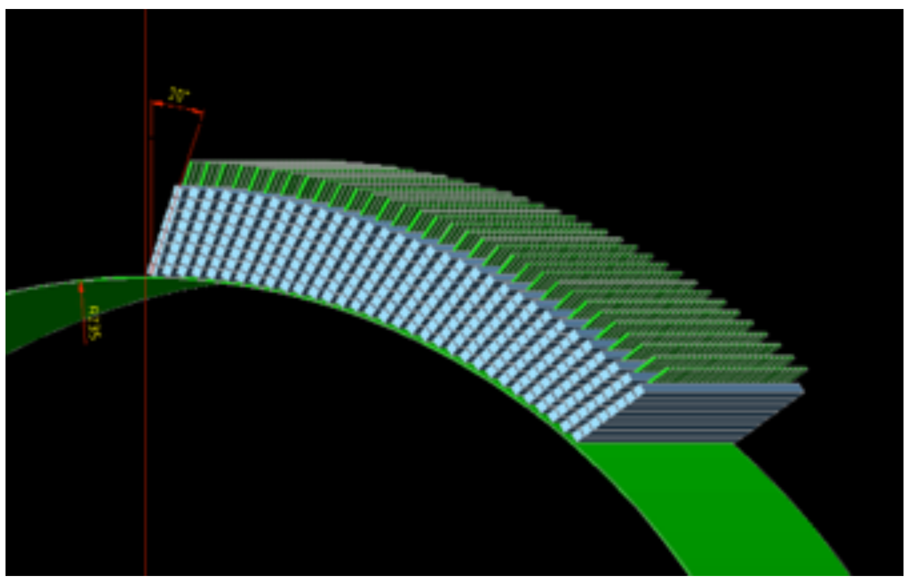

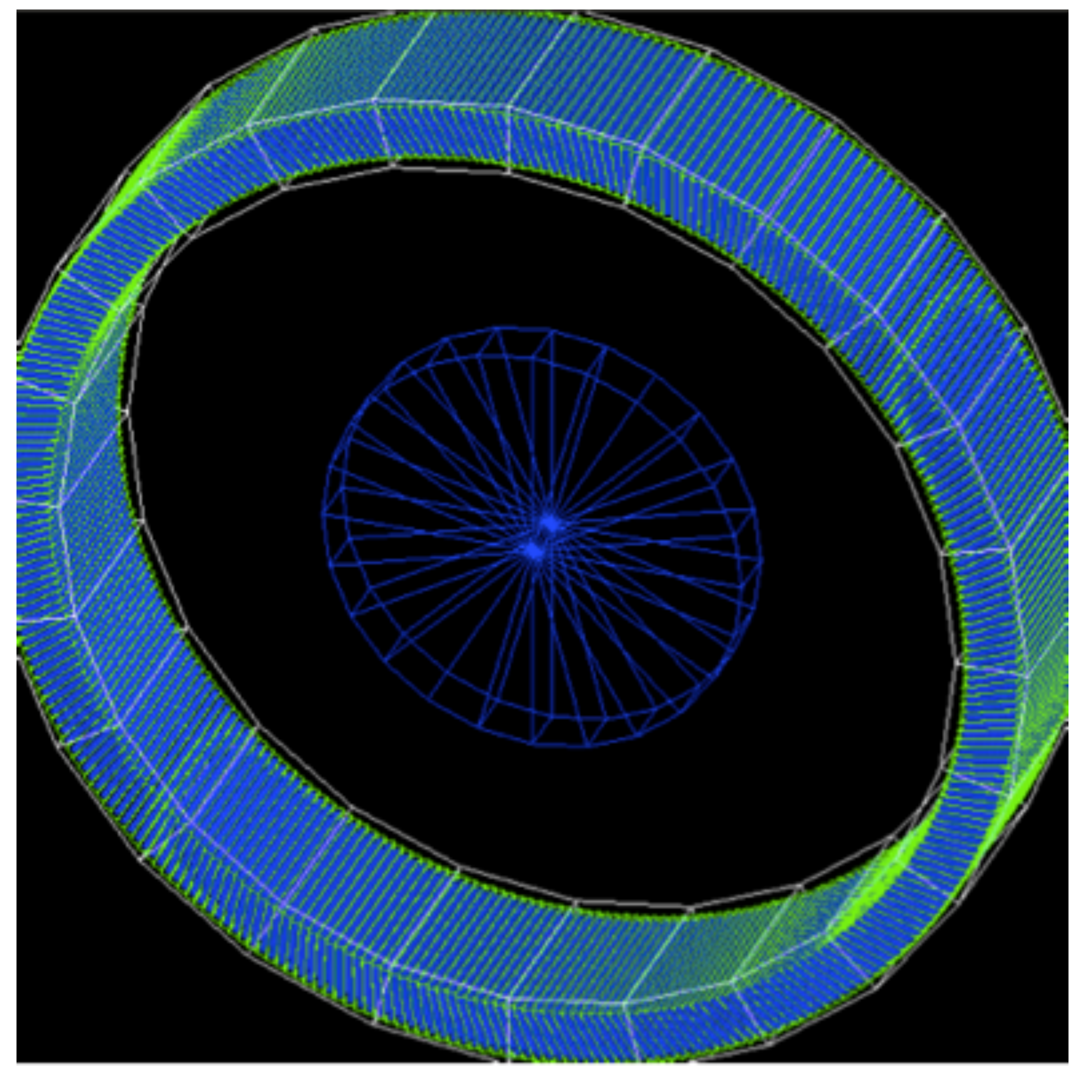

Novel design

- 20 degrees slanted layers.
- 300 layers arranged over a ring of 474 mm diameter.
- One module is the sum of 6 continuous layers.

AX-PET for brain imaging

- AX-PET was at the very beginning conceived for Brain Imaging (3x3 mm^2 crystal cross section, high axial resolution, etc).

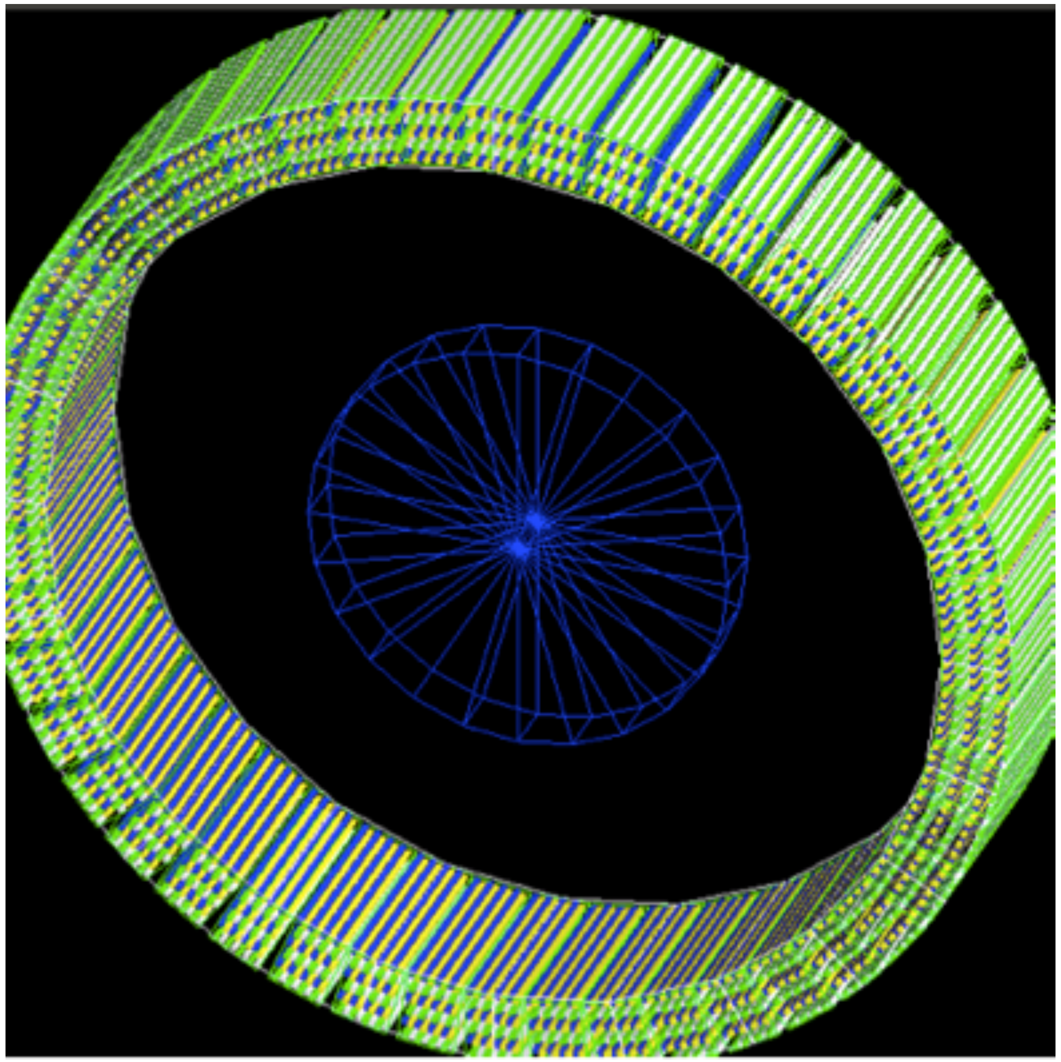

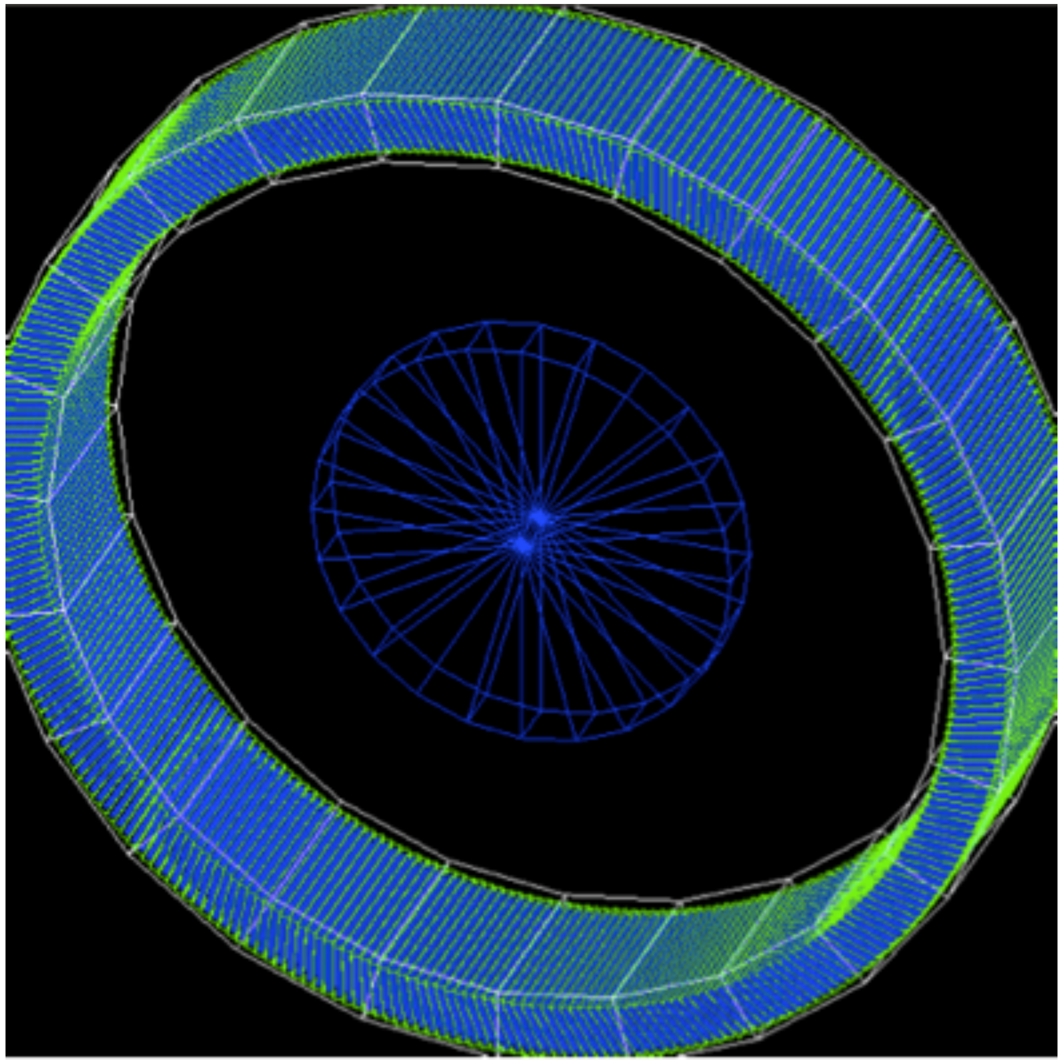

AX-PET for brain imaging

- The two geometries are comparable in terms of sensitivity.
- Reduced gaps translates into a more homogeneous sampling over the FOV.

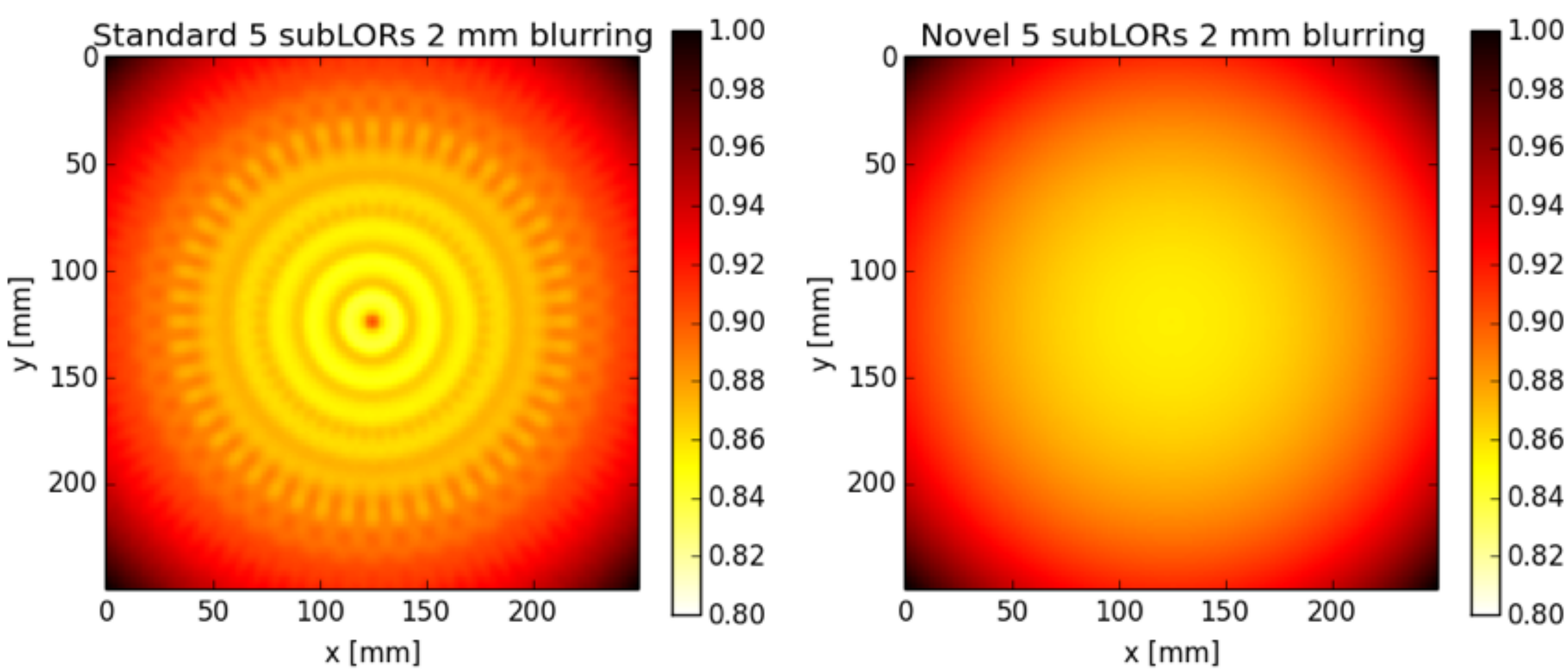

Cologne phantom

Resolution phantom

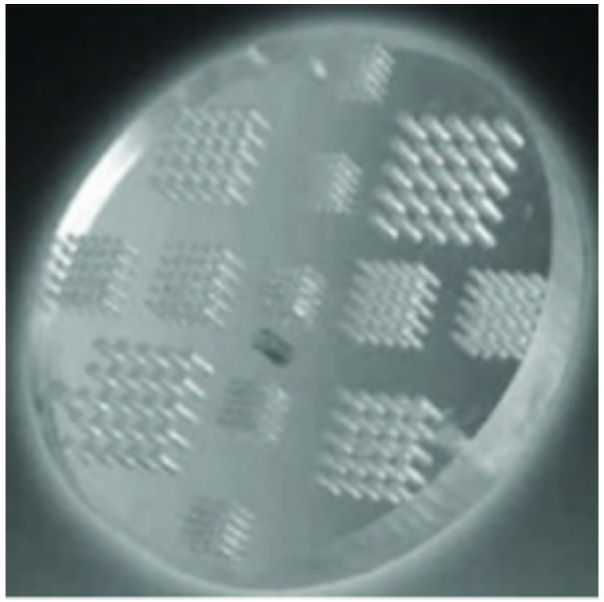

- 219 mm diameter lucite disk, 28 mm thick.
- Different rods of different diameters (2, 3 and 4 mm with 4, 6 and 8 mm pitch).
- 60 MBq activity in the phantom (close to NEC peak).

	Standard	Novel
Golden	998596	1011939
ICS	761360	868517

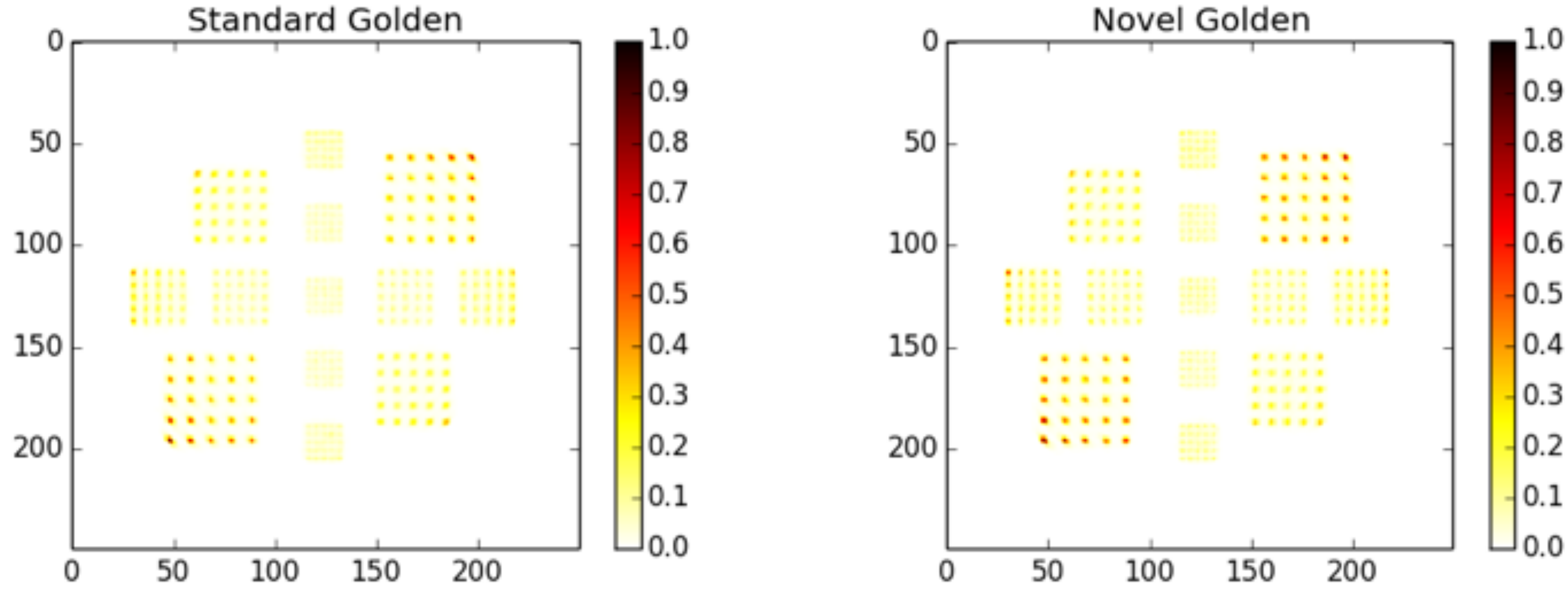

Images at iteration 10, 5subLORs, no attenuation correction.

Cologne phantom

Resolution phantom

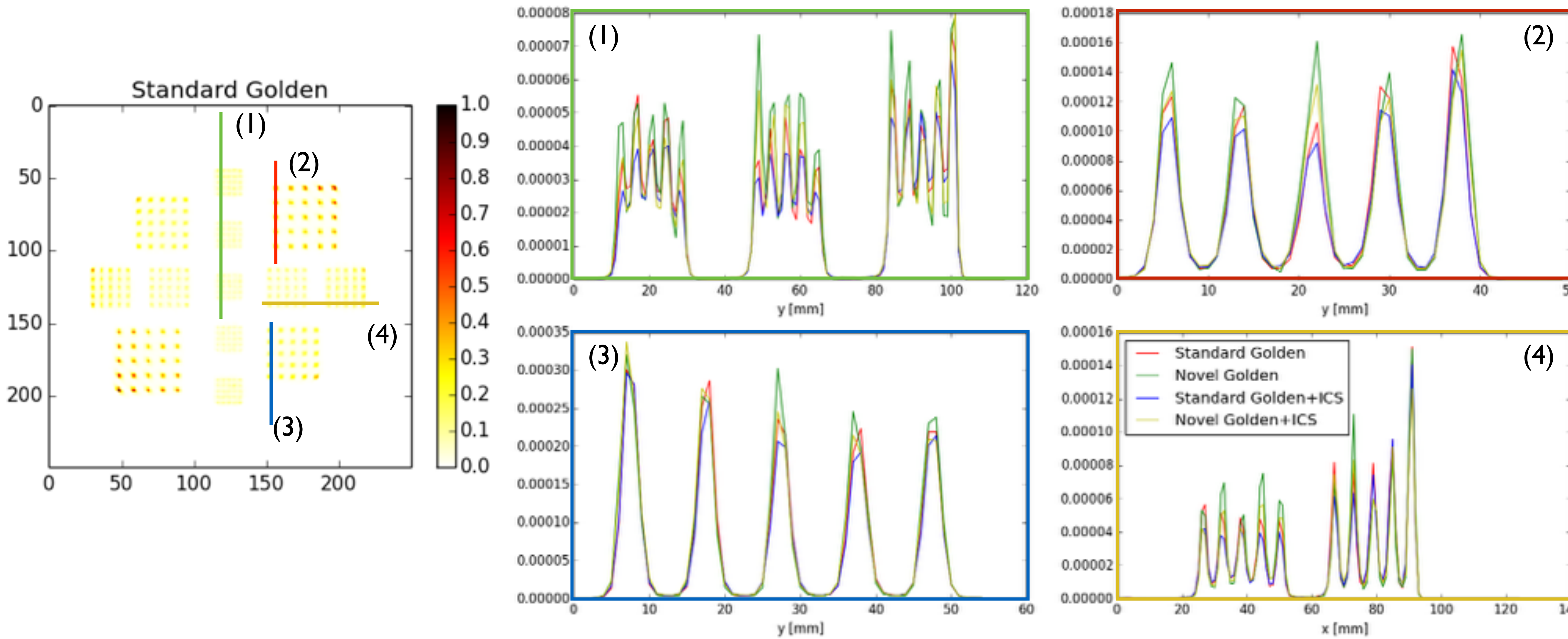

NEMA phantom

Image quality phantom

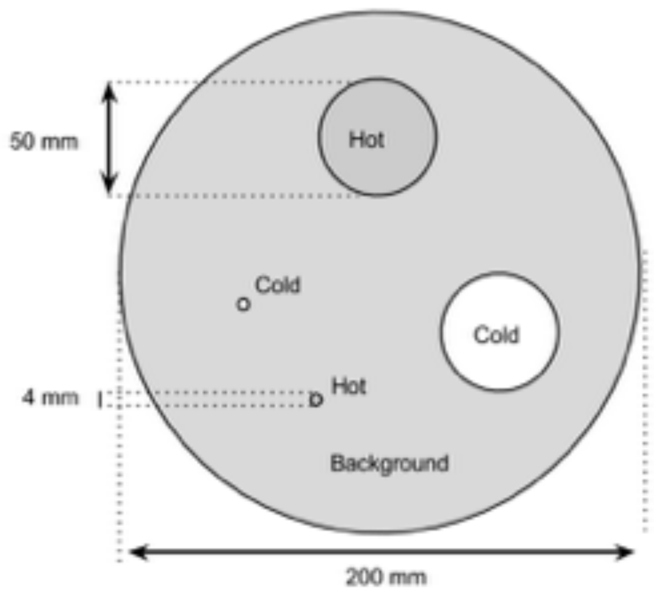

- 200 mm diameter air disk, 60 mm thick.
- Different rods (50 mm Hot-Cold, 4 mm Hot-Cold) in homogeneous background.
- Different activity ratios studied: 1.2:1, 5:1 and 20:1.
- 26 MBq total activity at the different ratios.

	Standard	Novel
Golden	2683442	2742472
ICS	2016631	2378176

5:1 ratio

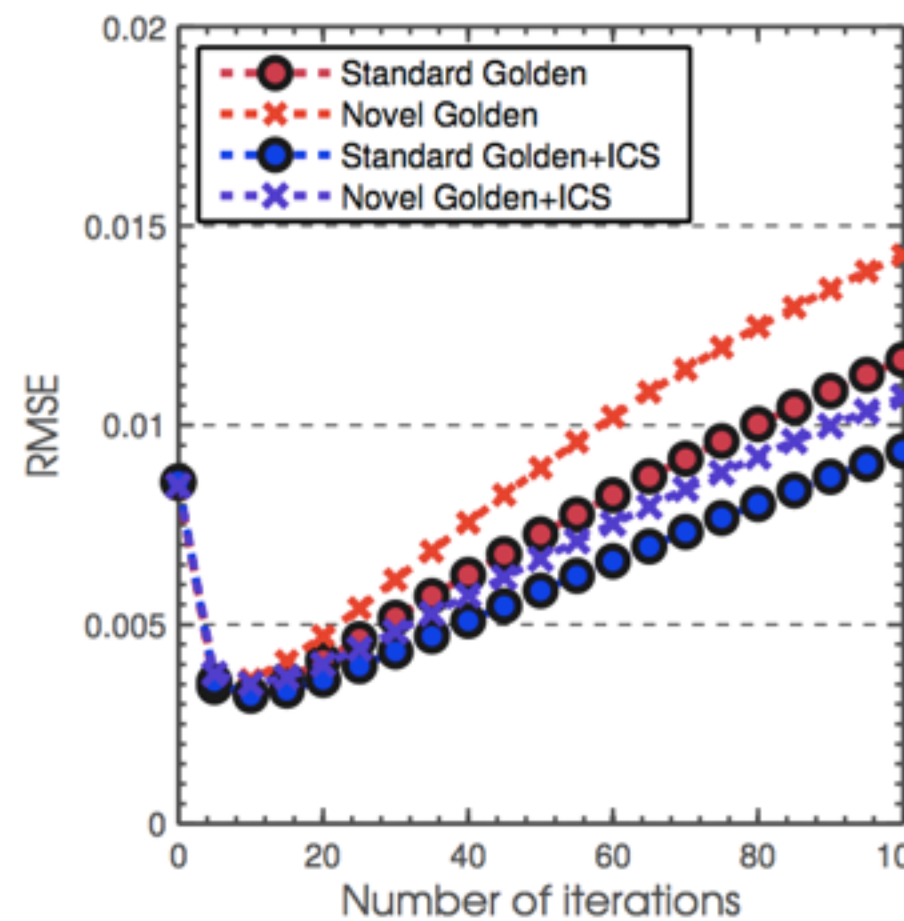

5:1 ratio

NEMA phantom

Image quality phantom

5:1 ratio

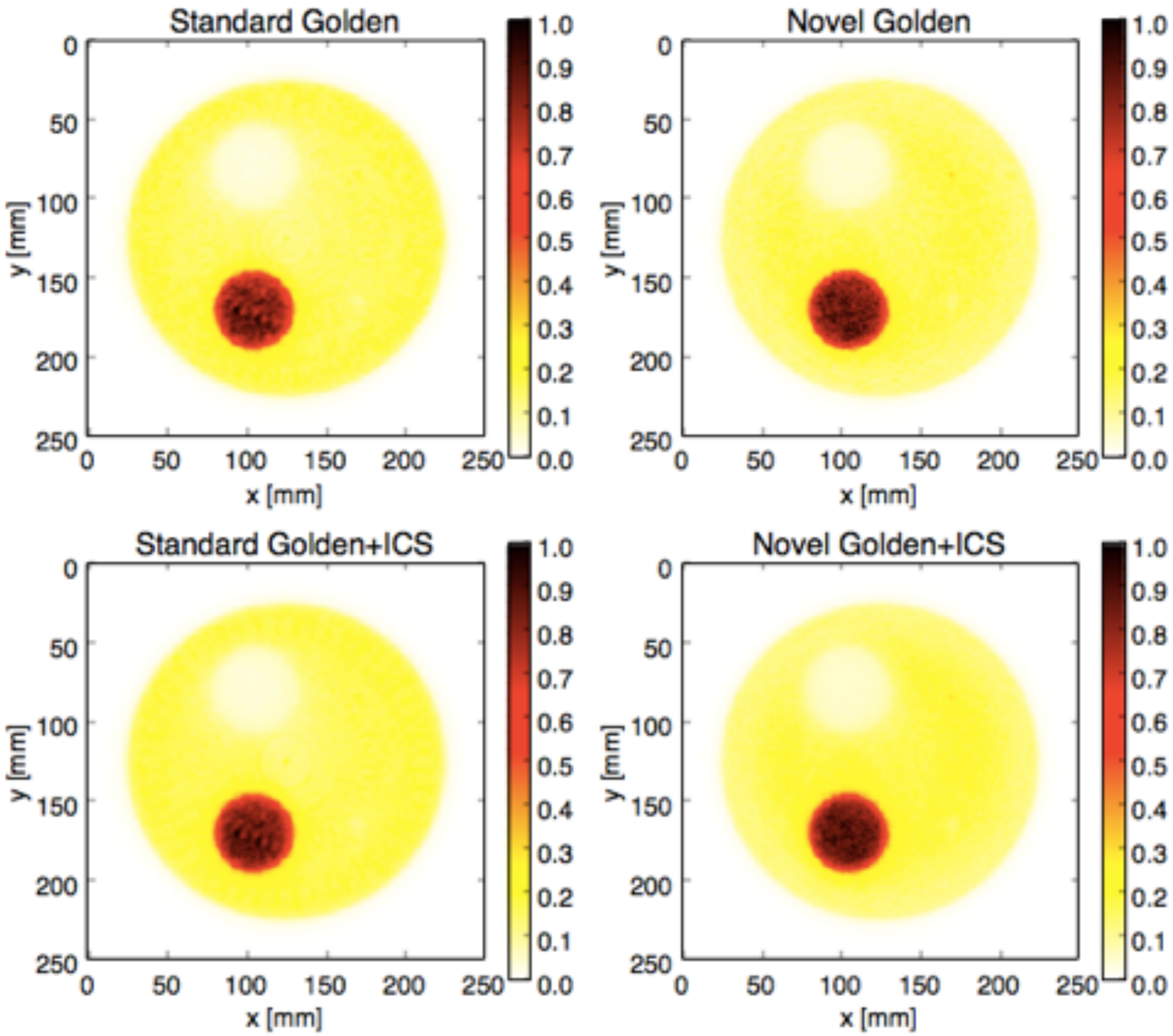

20:1 ratio

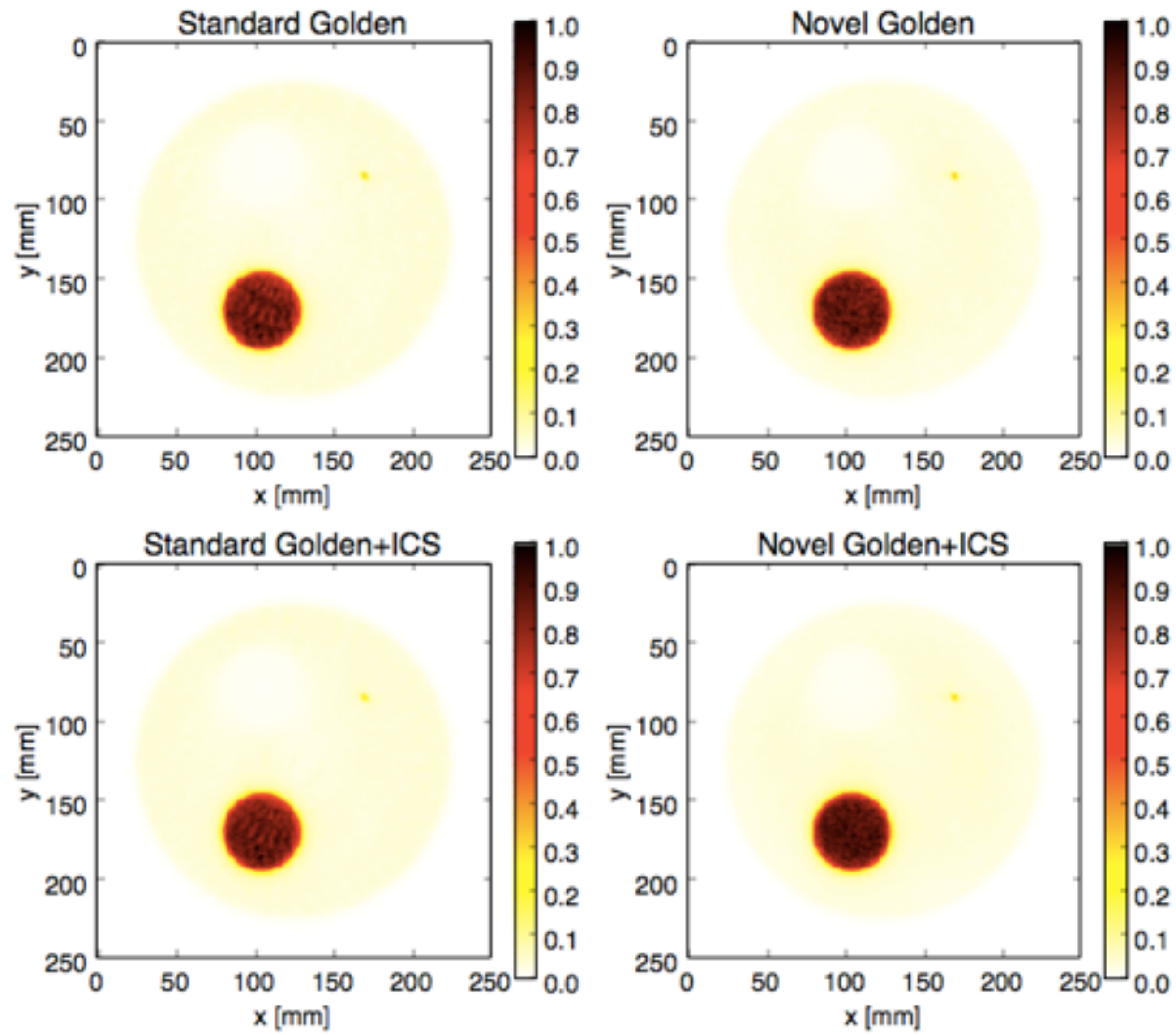

Iteration 10, 5 subLORs, random rejected.

Conclusions and Outlook

The collaboration accomplished with the primary objective:
- two modules built and fully characterized.

What we learned from simple source laboratory set-ups?
- spatial resolution 2 mm (x-y) and 1.35 mm (z).
- energy resolution 11.8% FWHM @ 511 keV.
- 3D localization of the gamma interaction.
- Large Compton Scatter fraction ~30%.

And from phantom measurements?
- AX-PET nicely works with extended sources and small animals, too.
- That every improvement in hardware has to be followed by at least the same effort in software development (Monte Carlo, new reconstruction algorithms) and usually it pays off.

AX-PET for brain imaging?
- Preliminary Monte Carlo studies are promising.
- Exquisite example of the AX-PET scalability.

AX-PET

Thanks for your attention!

Brain imaging challenges

- **Oncology**: brain tumors have 0.1% prevalence in western population, but among the most fatal cancers (malignant gliomas ~70%).
    - F18-FDG commonly used tracer, contrast can range from large necrotic tumor core lesion to low contrast small regions.
    - Tumors follow-up is usually characterized by SUV (~Activity concentration/ Injected dose) which is affected by RC and PVE, for lesiones below few times the system resolution.
    - The higher the resolution the better SUV is estimated.
- **Impairment Dementia**: life expectancy increases and with it dementia (WHO predict 48 million people in 2040 affected by dementia, AD mostly).
    - There is a huge variety of contrasts and lesion sizes related to AD.
    - Sensitivity is crucial to detect small lesions at early stages when treatments are still possible.

Individual analogue readout of MPPC output
Custom designed DAQ system

- **fully analogue** readout chain
- **not optimized** at all for this specific application

- **Amplifiers:** OPA486 (Lyso) / OPA487 (WLS)
- Fast **energy sum** for all the crystals in the module
- **VATA GP5 chip**
  - 128 ch charge sensitive integrating
  - fast (~ 50ns shaper + discriminator) / slow (~ 250ns shaper) branches
  - **sparse readout** mode: only the channels above thr are multiplexed into the output
- analogue info processed by custom made **VME ADC**

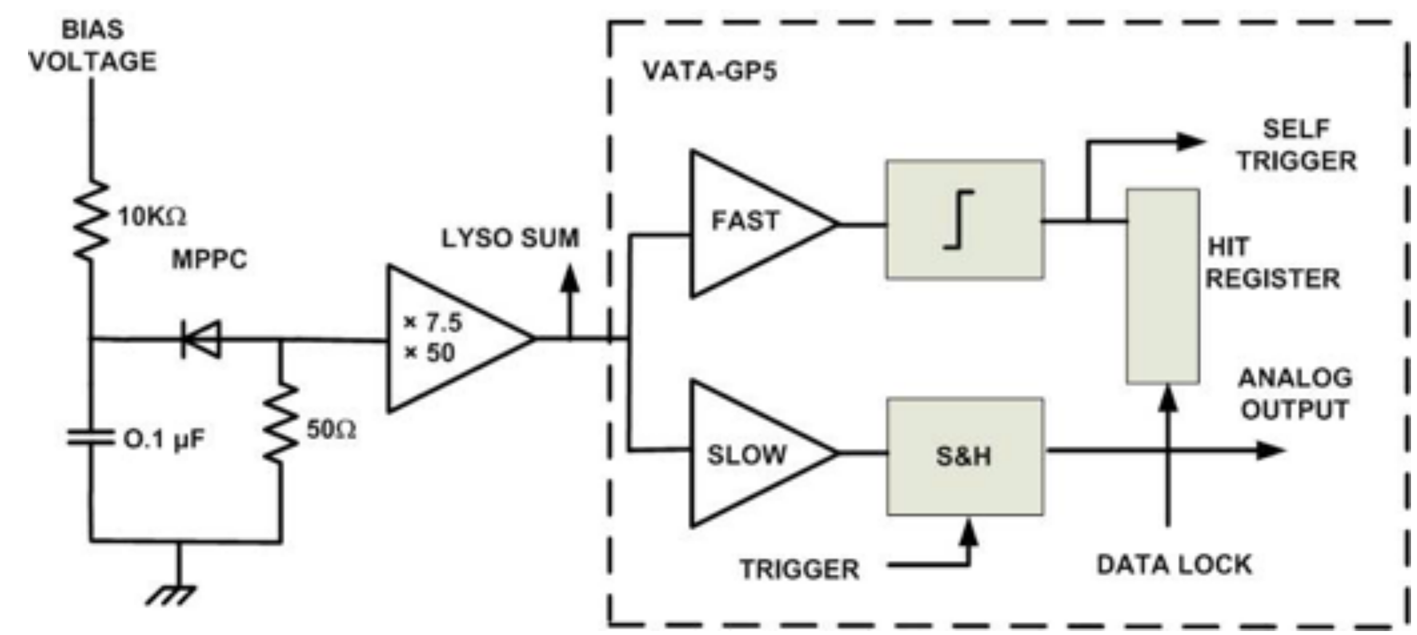

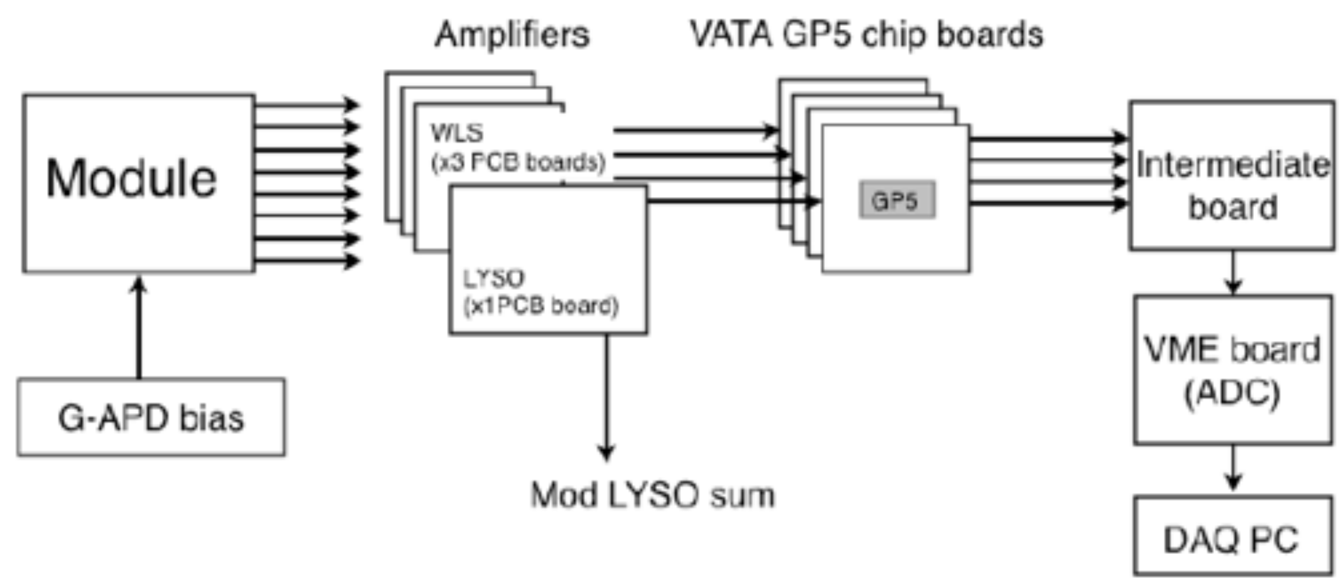

ICS reconstruction

System matrix element

$$n_j^{k+1} = \frac{n_j^k}{\sum_{i=0}^{I} a_{ij}} \sum_{i \in M} \frac{a_{ij}}{\sum_{j=0}^{J} a_{ij} n_j^k}$$

Sensitivity or normalization s_j

Image at iteration k

And what if a_{ij} is a Triple $a_{i'j}$?

Conventional approach → Identification

$$\frac{a_{i'j}}{\sum_{j=0}^{J} a_{i'j} n_j^k} = \frac{a_{i_t j}}{\sum_{j=0}^{J} a_{i_t j} n_j^k}$$

- One of the 2 LOR is selected, (t =1 or 2).
- In **this study**, **randomized selection** is used.

Our approach → V-projection

$$a_{i'j} = \eta_1 a_{i_1 j} + \eta_2 a_{i_2 j}$$

- Both LORs are kept but weights are assigned.
- In **this study, η_t = 0.5** equivalent to randomized selection.